Department of the Navy
Bureau of Ships
Contract Nonr-220(12)

PRESSURE DISTRIBUTION ON A HYDROFOIL RUNNING NEAR THE WATER SURFACE

Blaine R. Parkin
Byrne Perry
T. Yao-tsu Wu

This research was carried out under the Bureau of Ships
Fundamental Hydromechanics Research Program
Project NS 715-102, David Taylor Model Basin

Hydrodynamics Laboratory
California Institute of Technology
Pasadena, California

Report No. 47-2
April, 1955

Approved by:
M. S. Plesset

TABLE OF CONTENTS

ABSTRACT

The effect of the free surface on the pressure distribution on the upper side of a shallow-running hydrofoil is considered from a general point of view. Previous theoretical and experimental work is reviewed in order to compare the range of flow variables for which each treatment of the surface proximity problem is valid. A qualitative theoretical expression for the pressure is developed. This result shows the relative importance of the pertinent parameters and it is shown to agree qualitatively with previous experiments as well as with new pressure measurements made in the Free Surface Water Tunnel. The above considerations reinforce the view generally held in the past, that the methods of potential theory when properly applied to hydrofoils at shallow submergences may be expected to lead to valid and useful results.

I. INTRODUCTION

The hydrodynamics of hydrofoils has become a matter of renewed interest in recent years because of their potentialities in the design of small craft.[1] Such hydrofoils differ from conventional hulls in that they obtain their lift by hydrodynamic action rather than by hydrostatic buoyancy. In this regard they are closely related to planing surfaces and airfoils. When deeply submerged, in fact, the hydrofoil has a flow pattern which is identical with that of an airfoil of the same geometry moving at the same Reynolds number. It seems logical, therefore, to start any theoretical or experimental study of hydrofoils by using methods which are well-known and widely utilized in aerodynamics. Thus, for example, the effects of aspect ratio, attack angle, or Reynolds number, may be readily understood. It is supposed, in this approach, which is the customary one, that the effect of the water surface on the flow can be taken into account as a correction, much the same as the ground effect or tunnel wall corrections might be done on an airfoil.

On the other hand, one might ask if perhaps the free water surface does not introduce critical phenomena in such a way that the aerodynamic picture of the flow is not even a good first approximation, or perhaps while valid enough in some regimes, it fails completely in others. That such is the case has been strongly suggested by some recent experimental and theoretical work[2, 3, 4] where it was found that the pressure on a hydrofoil near the surface is severely limited, and that the total lift drops to zero as the profile approaches the surface. It has been asserted, therefore, that the aerodynamic approach must be replaced by other considerations which account for these discrepancies, and that any theory not so constructed is invalid.

While this may indeed be the case for some very low ranges of the speed, it will be made clear herein that for the range of speed which is of practical interest, the conventional approach to the problem is perfectly satisfactory. The purpose of this report, therefore, is to explore in a general way the behavior of the flow about a shallowly submerged hydrofoil so that the principles governing such a flow will be clarified.

II. BACKGROUND DISCUSSION

Perhaps the easiest way to understand the problems which are likely to arise in connection with the behavior of a hydrofoil near the water surface is to observe experimentally the various regimes of the flow. In Figs. 1 to 5 are displayed a variety of flow configurations on a two-dimensional hydrofoil (see Appendix A), which will now be described qualitatively in order to provide background for subsequent discussion. While a relatively complex variety of flow phenomena occur, there are essentially two principal regimes of flow, according as the Froude number* is high or low.

In the first, which may be expected at high Froude numbers, the flow is smooth over the upper hydrofoil surface, and no discontinuities occur on the free surface (Figures 1a, 2a,b,c,d, and 3a). This type of flow has been widely observed on actual hydrofoils and has been assumed as a starting point for nearly every theoretical treatment. If the foil in the high Froude number regime approaches the surface too closely, however, there will very likely be some air ventilation and a consequent complete separation of the flow over the upper surface as shown in Figures 2e and 3b. In this configuration the hydrofoil is actually operating more like a planing surface, since if the speed-depth ratio (Froude number) is high enough, the whole upper surface will be unwetted, and the spray sheet will shoot off in an upward or even reversed direction, very much as in those planing flows which were studied by Green.[5] Practical foils are designed to avoid this condition by always running at a reasonable submergence.

In the second major regime of flow the surface is broken by various types of gravity waves or hydraulic jumps, as shown for example in Figs. 1b, 4, and 5. These flows occur at low Froude numbers, as might be expected, and result in considerably different conditions so far as the forces and pressures on the hydrofoil are concerned.

It is clear of course, as pointed out by Laitone,[4] that if the submergence of the hydrofoil is very small, the flow over the aft end of the upper surface can be treated as though it is in a slightly sloping open channel and the widely known channel effects such as hydraulic jumps may be expected to appear. Thus, as shown in Fig. 4c, a standing wave may occur slightly ahead of the hydrofoil and another may also appear further aft along the chord.

*Based on profile chord length.

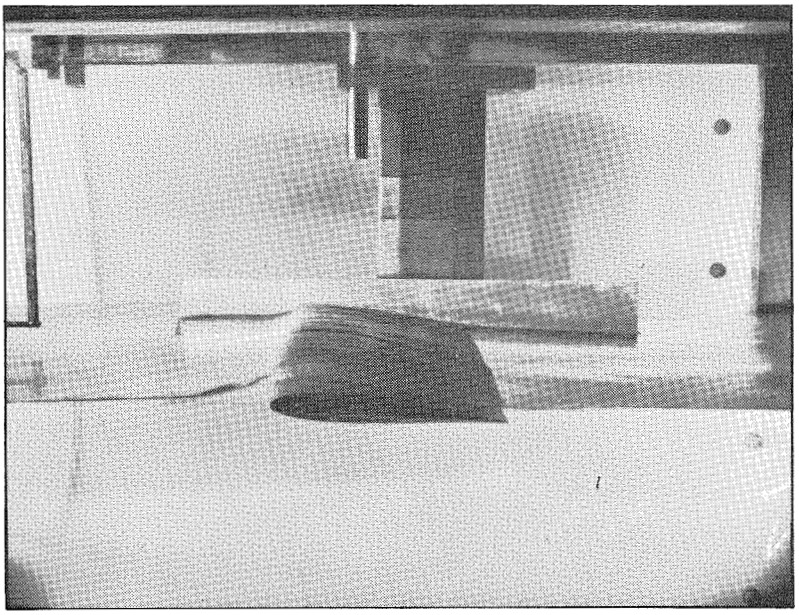

(a) High Froude number.

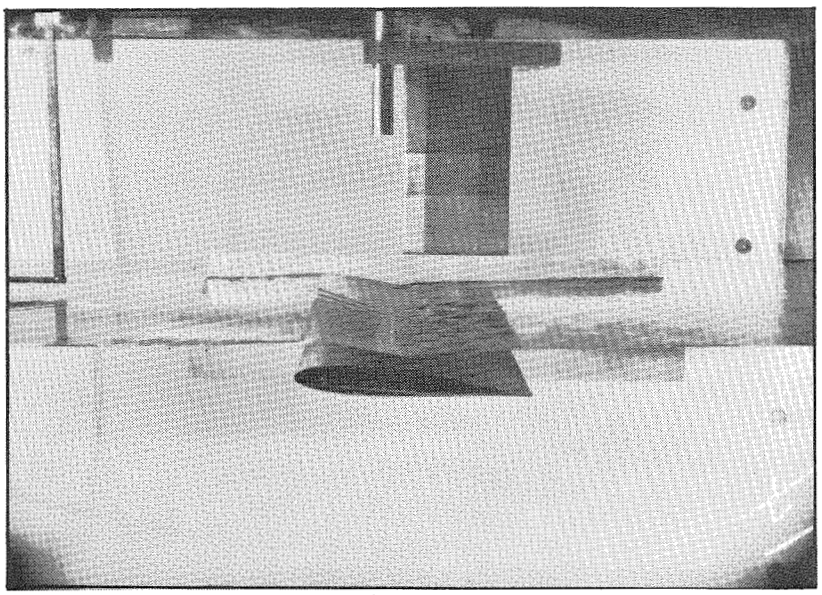

(b) Low Froude number.

Fig. 1

The two principal regimes of flow for shallowly submerged hydrofoils.

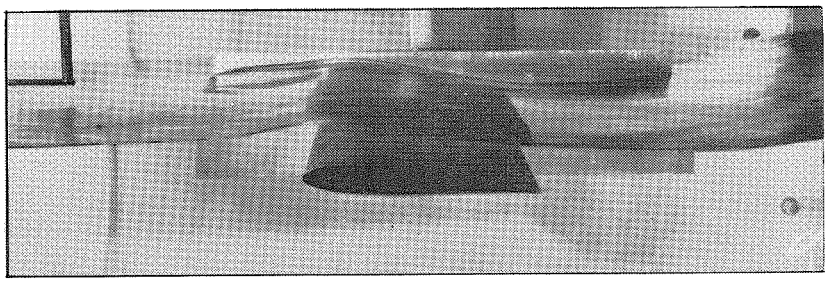

(a) U = 3.61 fps h/c = .280

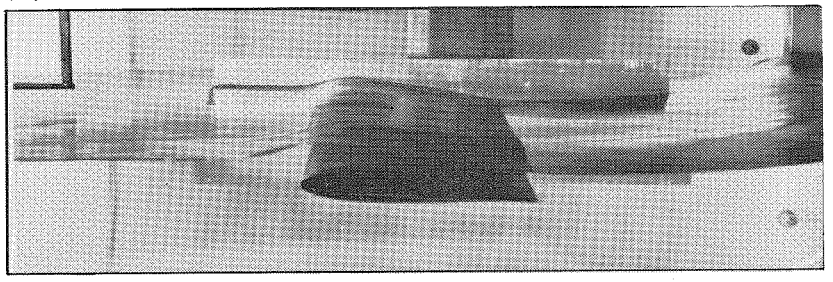

(b) U = 3.61 fps h/c = .148

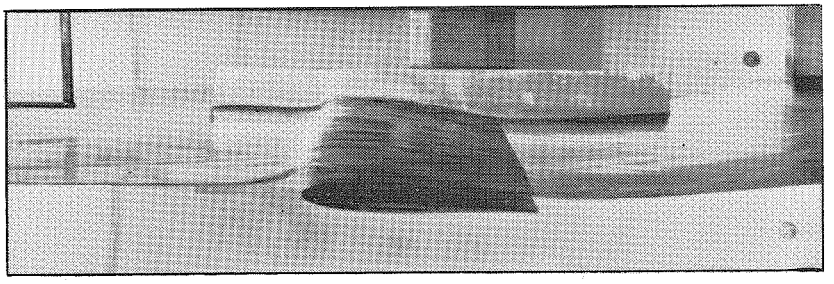

(c) U = 3.58 fps h/c = .092

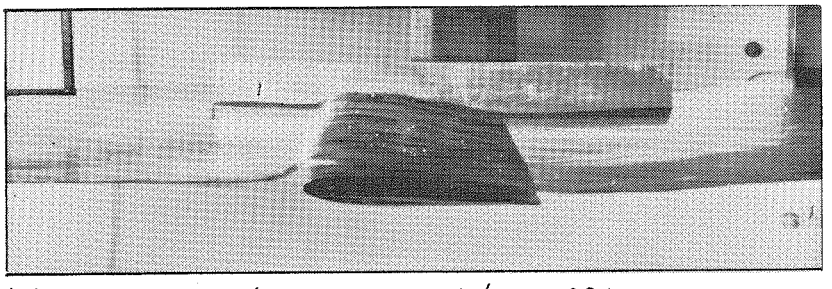

(d) U = 3.69 fps h/c = .084

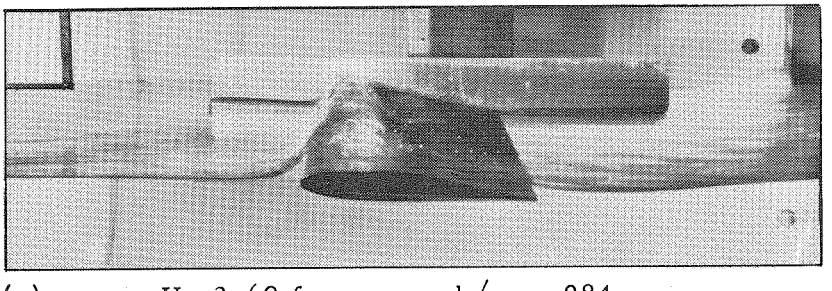

(e) U = 3.69 fps h/c = .084

Fig. 2

The influence of submergence on hydrofoil ventilation.

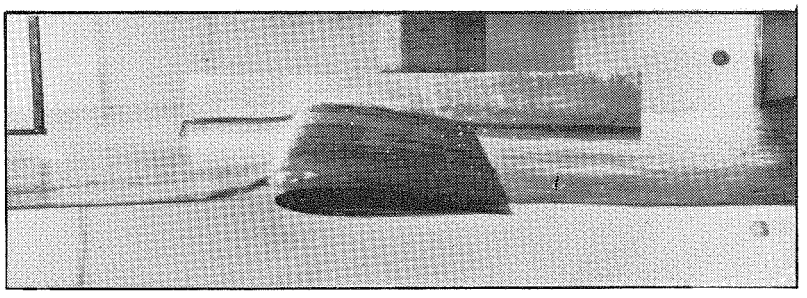

(a) U = 4.22 fps h/c = .148

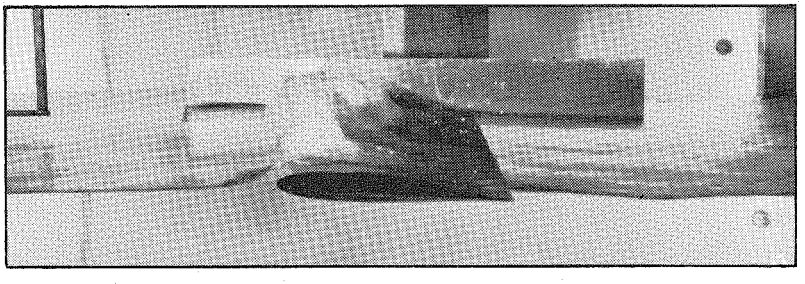

(b) U = 4.22 fps h/c = .148

Fig. 3

Nonventilating and ventilating flows at high Froude number.

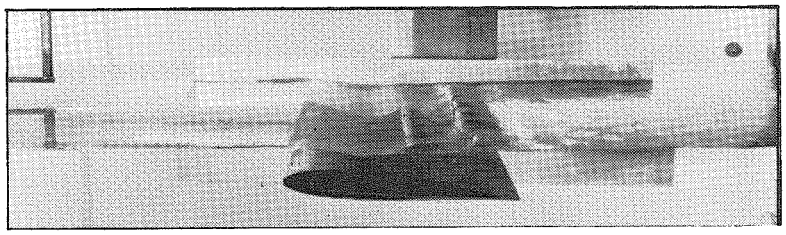

(a) U = .948 fps h/c = .197

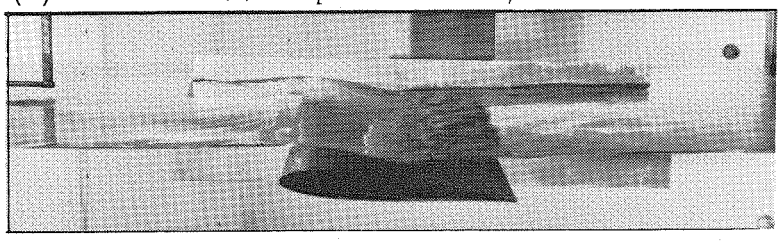

(b) U = 1.433 fps h/c = .187

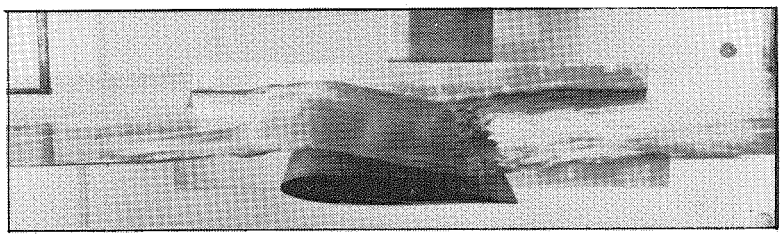

(c) U = 2.27 fps h/c = .169

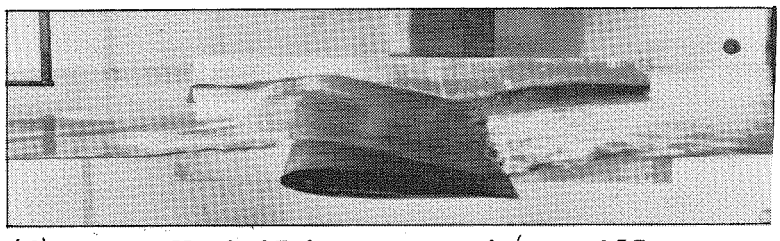

(d) U = 2.27 fps h/c = .157

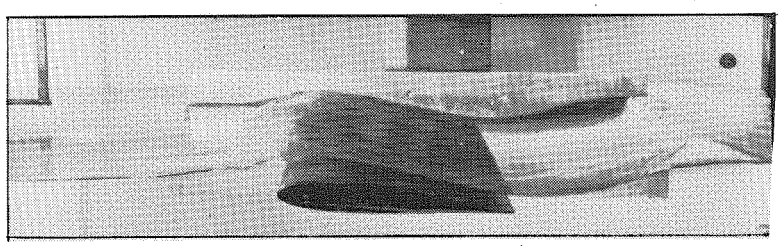

(e) U = 2.78 fps h/c = .136

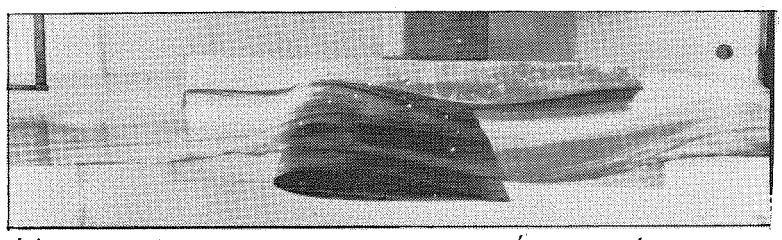

(f) U = 2.78 fps h/c = .136

Fig. 4

Effect of increased Froude number.

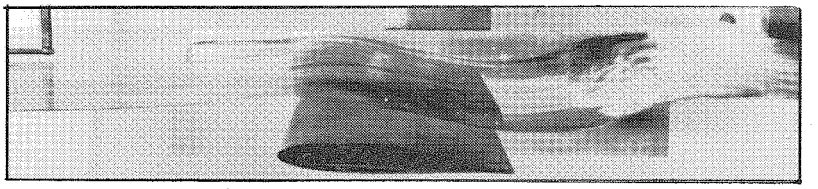

(a) U = 2.81 fps h/c = .252

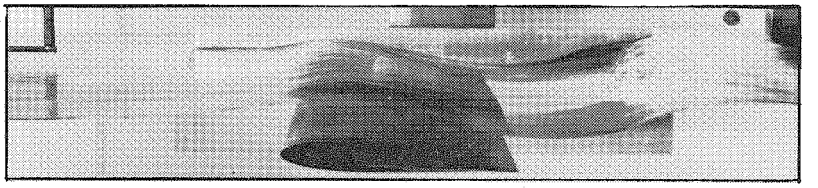

(b) U = 2.83 fps h/c = .208

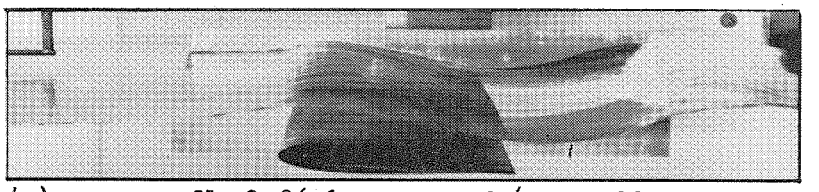

(c) U = 2.86 fps h/c = .189

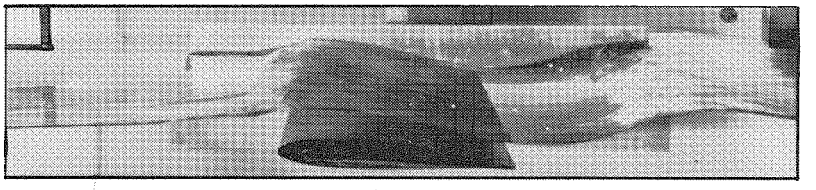

(d) U = 2.78 fps h/c = .172

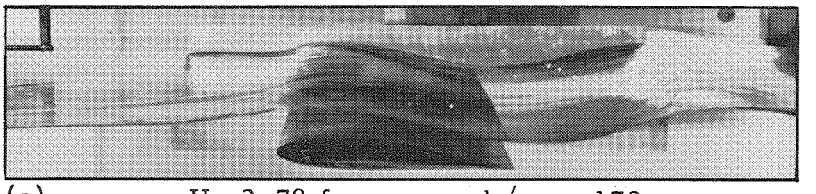

(e) U = 2.78 fps h/c = .172

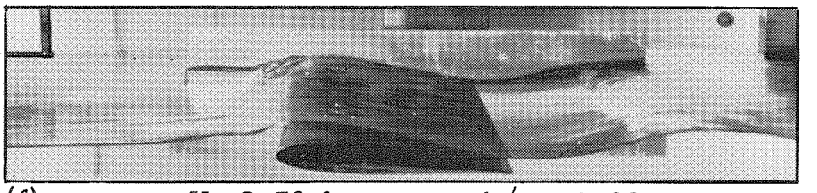

(f) U = 2.78 fps h/c = 1.08

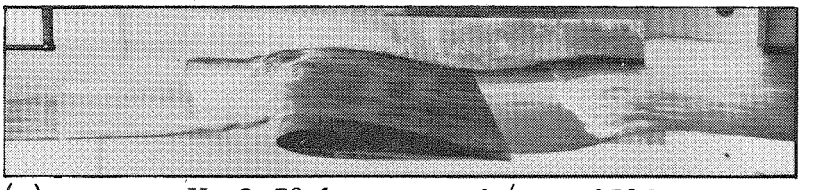

(g) U = 2.78 fps h/c = .0787

Fig. 5

Effect of submergence is shown in this series.

At higher speeds these will be swept away when the velocity of flow over the upper surface exceeds that for which standing waves can occur. So far no exact criteria have been established as to the dividing point between the high and low Froude numbers, but it seems likely that it is closely related to the known effects of channel velocity on the propagation of two-dimensional channel waves.

From this discussion it will be seen that the flow over a shallowly submerged foil will display characteristics of one type or another, either smooth or characterized by standing jumps and waves, depending on the Froude number. It is important to realize, however, that the practical application of foils ordinarily requires that, first, they run at considerable depth where surface effects are not of primary importance, and second, since the hydrofoil obtains its lift by dynamic action, it is implied that the Froude number will be relatively high. It is this last point that needs to be emphasized, since it indicates that the various wave phenomena concomitant to low Froude numbers are mainly of academic interest. The practical problem is to calculate the characteristics of hydrofoils near the surface when the Froude number is high and the flow over the upper surface is therefore smooth.

The theory of hydrofoils running near the water surface is by no means new, but all of the early investigations were concerned with calculating the over-all forces on the hydrofoil, namely the lift and drag, rather than the details of the local flow. Important examples of such work were the theory of two-dimensional hydrofoils carried out by Keldysch and Lavrentiev,[6] Weinig,[7] and Wladimirov.[8] These works, however, contain various approximations or over-simplifications which make it difficult to apply them to practical problems with any accuracy. In particular, the theory of Keldysch and Lavrentiev cannot be used for hydrofoil submergences of less than one-half chord length because of certain physical assumptions, necessitated by the linearization scheme, which in turn result in mathematical difficulties involving convergence. These restrictions were noted by Wladimirov,[8] and they are typical of all linearized theories. It seems desirable to take note of such difficulties here because there have been some recent attempts to use the theoretical formulas without proper regard for this limitation.

To extend the previous work and remove some of the restrictions necessary in applying the previously obtained formulas, the forces on a three-dimensional hydrofoil of high aspect ratio have been recently calculated by Wu.[9] Here the hydrofoil problem is formulated in a manner similar to the lifting line wing theory of L. Prandtl and the free surface effect is included with a first order linearization. The solution is considerably improved over earlier works by the inclusion of the effect of gravity in the form of appropriate wave potentials, and the calculation is further extended so that the spanwise lift distribution may be arbitrary. It is not our intention to discuss this theory in detail here, but an example of the kind of practical results which can be computed from it are shown in Fig. 6 along with some force measurements[10] from a towing tank for comparison, (the calculations are described in Appendix B). It can be seen that the agreement between theory and experiment is good and that all the trends are properly predicted by the theory, even for submergences as small as one-half chord length. Since most practical hydrofoils will undoubtedly run at somewhat deeper submergences, it seems reasonable to assume that this theory should suffice to predict the free surface effect on the forces in most cases of practical interest.

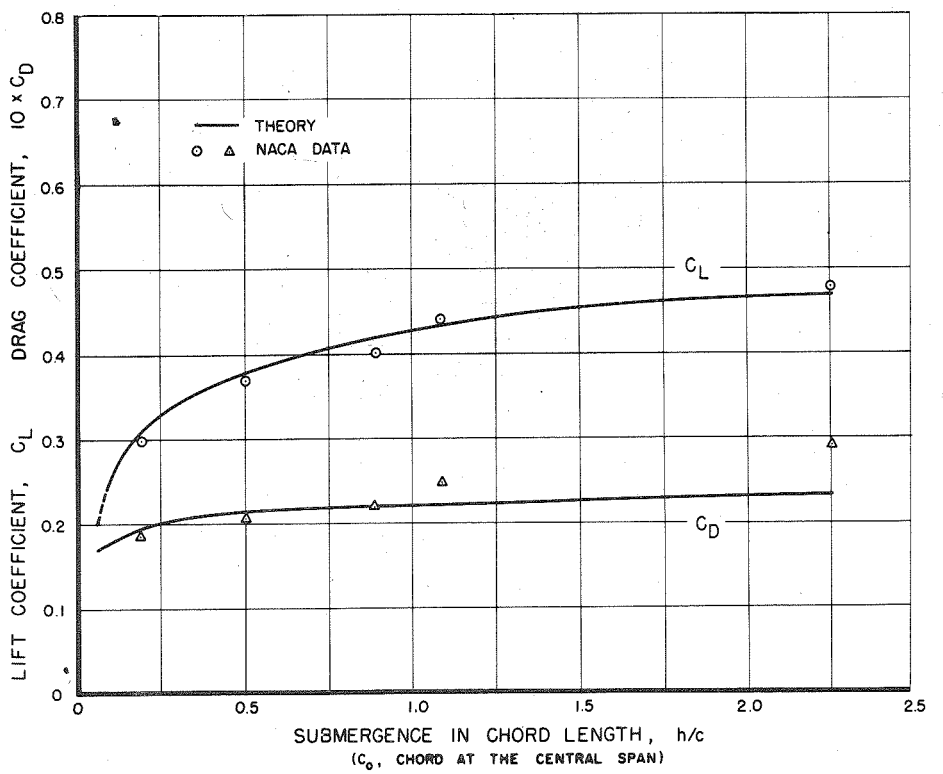

Fig. 6

Besides its effect on the forces on the hydrofoil, the free surface also influences the pressure distribution. It is of practical importance to know the magnitude of this effect since it determines the way the cavitation characteristics of the hydrofoil may be altered by the presence of the free surface. For three-dimensional hydrofoils which are not too near the free surface, the theory[9] just described can in principle be used to consider the first order change in pressure distribution in accordance with the usual lifting line approximations. In this approach it is supposed that the flow at any spanwise section is essentially two-dimensional and that the flow direction at infinity is altered by the amount of the so-called downwash angle. Thus, if two-dimensional section data is available for the profile at any particular spanwise section as a function of angle of attack, the three-dimensional pressure distribution can be readily computed by taking into account the downwash correction. If, however, the hydrofoil is very near the free surface, say within less than one chord, the lifting line image system would would probably have to be modified to obtain accurate results by distributing the vorticity in a chordwise manner as well as in the spanwise direction. While Keldysch and Lavrentiev[6] distributed the vorticity along the chord in their two-dimensional theory, they did not carry out calculations for the pressure and moreover, as mentioned previously, their results are not applicable for small submergences. It would of course be of considerable interest to investigate further their general theoretical line of attack to eliminate if possible some of the discrepancies encountered to date, but no discussion of such matters can be given here.

The pressure distribution problem has also been worked on from the experimental side in a recent program by Ausman.[2, 3] In his measurements, which appear to be the first of the pressure on a hydrofoil in the presence of a free surface, considerable data were obtained for the NACA 4412 profile of 6 in. chord, over a range of attack angles and submergences. The hydrofoil was mounted in a circulating water channel so that it was held stationary with the water moving past it. While the tests were made at rather low speeds, that is, low Froude numbers, they appear to be reasonably precise.

A typical set of data of the type taken by Ausman is shown in Fig. 7. Here are shown a series of pressure distributions taken at nearly the same speed with a fixed value of the geometrical angle of attack of 10^{o}. The parameter which is varied is the submergence of the trailing edge below the

undisturbed water surface. Ausman found that the pressure coefficient on the upper surface of the profile did not reach nearly so low a value as would be obtained if the hydrofoil were running deeply submerged. It was further noticed by Ausman that as the hydrofoil approached the surface the smooth wave pattern observed for deep running was replaced by a sharp discontinuity in the free surface which he called a hydraulic jump. A similar effect observed in the free surface tunnel is shown in Fig. 1b. The term "jump" appears to be appropriate for this phenomenon because it resembles very markedly the hydraulic jumps which are observed in two-dimensional channels of shallow slope.[11, 12]

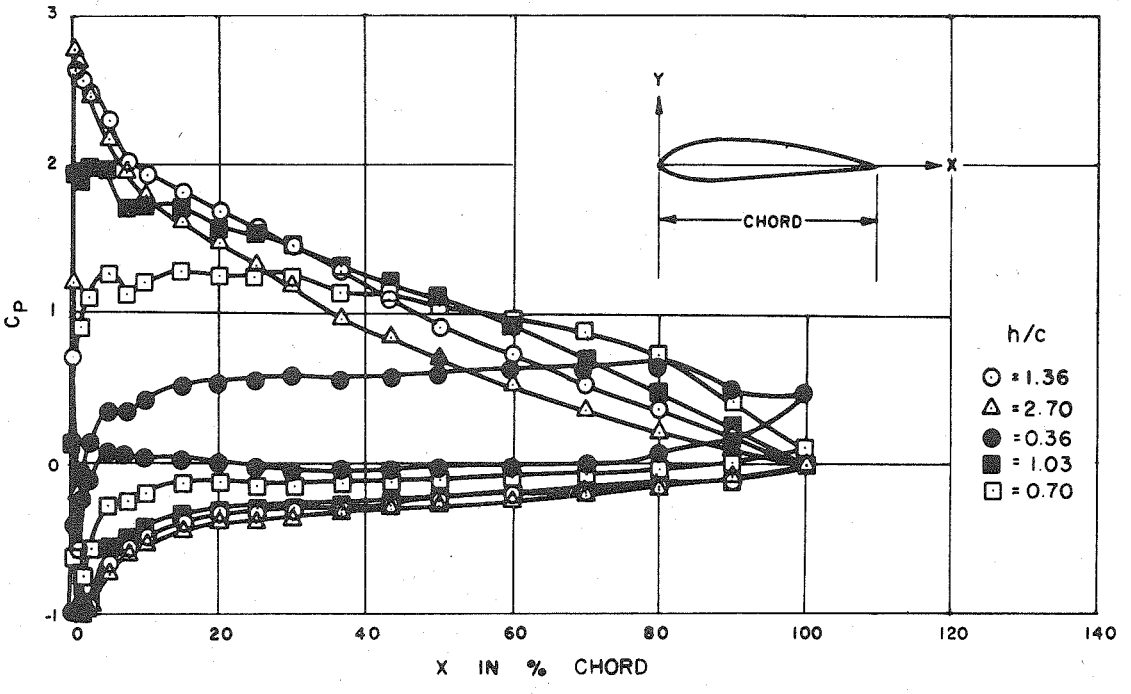

Fig. 7

On the basis of this resemblance, Laitone[4] developed some theoretical relationships which in part explain Ausman's observations. Laitone assumes that the hydrofoil is very shallowly submerged and that the pressure is distributed hydrostatically. This latter assumption is equivalent to assuming that the hydrofoil is running at a very low Froude number $U/\sqrt{gc}$. By further supposing that the upper hydrofoil surface is nearly horizontal, Laitone calculates the minimum pressure coefficient to be $C_{p_{min}} = -gh/U^2$ by use of some known relationships from one-dimensional channel theory. It must be emphasized that Laitone's theory is valid only for extremely small Froude numbers.

The chief result of Ausman's experimental work and Laitone's theory can perhaps be summed up by the single graph shown in Fig. 8.

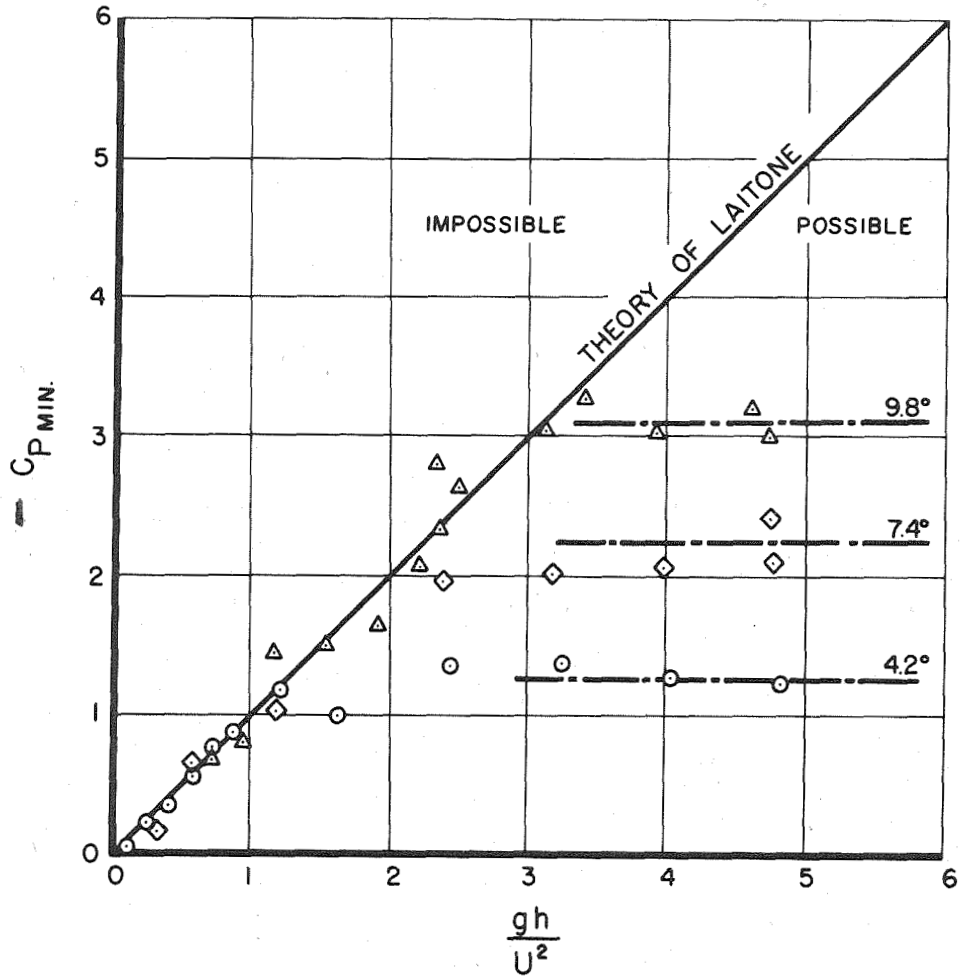

Fig. 8

According to Laitone's theory, the pressure coefficient is so limited in value by the presence of the free surface that it cannot take on any of the values shown to the left of the line $C_{p\,min} = -gh/U^2$, which in a sense is therefore a barrier to the left of which the data cannot lie. Some typical results from Ausman's experiments are plotted on this graph and it can be seen that in fact they do not cross the barrier with the possible exception of a few points which were run near the critical speed of the water channel and are, therefore, inaccurate. It appears to the present writers that Ausman's experiments and Laitone's theory give a reasonable picture of a certain limiting effect which occurs at small Froude number. It will be shown in the following section, however, that this limiting effect by no means exists in regions of higher Froude number.

III. QUALITATIVE HYDROFOIL THEORY FOR SHALLOW SUBMERGENCE

Let us consider a two-dimensional hydrofoil at small angles of attack submerged at depth h of the order of, or less than the chord length c from the free surface of infinitely deep water. The coordinate system chosen is shown in Fig. 9. The flow velocity U at upstream infinity is taken to be constant. At any point in the water, we further adopt curvilinear coordinates (s, n) along and perpendicular to the streamlines, respectively. The fluid is assumed to be nonviscous, and the flow irrotational.

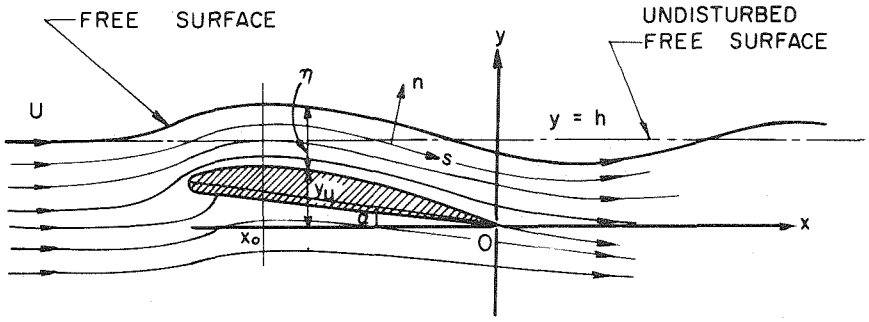

Fig. 9

The condition of irrotationality is expressed as

$$\frac{\partial q}{\partial n} = -\frac{q}{r} \tag{1}$$

where q is the flow speed and r the radius of curvature of the streamline. The pressure of the liquid is given by Bernoulli's equation

$$p + \frac{1}{2}\rho q^2 + \rho g y = p_o \tag{2}$$

where the constant p_o holds everywhere through the liquid.

There are three boundary conditions for this problem:

$$\begin{aligned} &1.\ \vec{q} \cdot \vec{n} = 0 \text{ on the profile;} \\ &2.\ \vec{q} \cdot \vec{n} = 0 \text{ and } p = p_o \text{ on the free surface;} \\ &3.\ \text{the Kutta condition at the trailing edge.} \end{aligned} \tag{3}$$

The exact solution to this system of equations is rather difficult to obtain. However, if the free surface elevation is known, one might calculate the pressure field with good accuracy by using some graphical method based on a network of flow meshes and integrating (1) numerically with known

boundary values (e.g. cf. Ref. 12, Art. 13, p. 54). Such computations will not be carried out here, but an attempt will be made in this section to give qualitative consideration to the various parameters which are of importance.

Writing all the physical quantities in nondimensional form, one would expect that the pressure coefficient, defined as*

$$C_p = \frac{p - p_\infty}{\frac{1}{2}\rho U^2}$$

depends in general on five dimensionless quantities

$$C_p = f\left(\frac{U}{\sqrt{gc}}, \frac{h}{c}, \frac{x}{c}, \frac{y_u}{c}, \alpha\right) \tag{4}$$

where y_u is the y-coordinate of the hydrofoil at x. Other equivalent arrangements of the dimensionless parameters are of course possible. The first term inside the parenthesis represents the gravitational effect and is the Froude number. The second term indicates the effect of submergence depth while the last two terms describe the geometry of the solid boundary. We shall calculate approximately the value of C_p over a part of the boundary so that the dependence of C_p on these variables can be exhibited.

We shall take a two-dimensional hydrofoil so located that α and h/c are small and consider only the region $x_o \leq x \leq 0$ on the upper side of the profile where dy_u/dx has small negative values. Then except for the case in which a hydraulic jump occurs inside this region (the Froude number for this condition is known from experiments to be very small), we can assume that the direction cosine (ℓ, m) of $\vec{n}$ is $m \approx 1$ and $\ell = 0(\alpha)$ so that $\partial/\partial n$ can be replaced by d/dy, and that the radius of curvature r of the streamlines depends on x only; that is,

$$r(x, y) \approx r(x) = R(x) \approx \left(\frac{d^2 y_u}{dx^2}\right)^{-1}, \tag{5}$$

where $R(x)$ is the radius of curvature of the upper surface profile at x.

---

*All notations are defined in Appendix C of this report.

These assumptions are, of course, well-supported by the observations at higher Froude numbers. Then Eq. (1) can be integrated to yield

$$q_u(x) = q_f(x) \exp\left[\frac{\eta(x)}{R(x)}\right] = q_f(x)\left[1 + \frac{\eta(x)}{R(x)} + \cdots\right] \qquad (6)$$

where q_u, q_f are the flow velocity at $y = y_u$ and $y = y_u + \eta$ respectively. The value of q_f can be obtained by applying Bernoulli's equation, Eq. (2), to the free surface at x to give

$$q_f = U^2\left[1 - \frac{2g}{U^2}(y_u + \eta - h)\right] \qquad (7)$$

The pressure coefficient C_p at the hydrofoil surface is defined as

$$C_p = \frac{p_u - p_\infty}{\frac{1}{2}\rho U^2} \qquad (8)$$

where $p_\infty = \rho g(h - y_u)$ is the hydrostatic pressure of the upstream flow at the same depth as point (x_u, y_u).* Combining these results, we obtain for the case $\eta \ll R$,

$$C_p = -\frac{2gh}{U^2}\left(1 - \frac{y_u + \eta}{h}\right) - \frac{2\eta}{R} + \frac{4\eta}{R}\frac{gh}{U^2}\left(\frac{y_u + \eta}{h} - 1\right) \qquad (9)$$

or

$$C_p = -\frac{2h}{c}\left[(F^{-2})\left(1 - \frac{y_u + \eta}{h}\right) + \left(\frac{\eta}{h}\right)\left(\frac{c}{R}\right) - 2\left(\frac{\eta}{R}\right)(F^{-2})\left(\frac{y_u + \eta}{h} - 1\right)\right] \qquad (9a)$$

where

$$F = U/\sqrt{gc}$$

is the Froude number.

This result is valid only under the conditions mentioned above, and it exhibits the dependence of C_p on the several parameters. In Eq. (9) R

---

*This is the customary definition and corresponds to the experimentally measured values given by Ausman, wind and water tunnel workers, and the present writers. Laitone's definition differs slightly but coincides with Eq. (8) for the point at the trailing edge.

is an intrinsic property of the profile, and y_u can be expressed in terms of α and the profile geometry. While η depends on α, y_u, x and h, its value is in general of the order of h. The first term on the right-hand side is essentially due to gravitational effects, while the second term, rewritten as $\eta/R = (\eta/h)(h/c)(c/R)$, depends mostly on the submergence depth (h/c) and the hydrodynamic pressure resulting from the curvature of the streamlines. The last term represents the higher order nonlinear effects.

When F and α are held constant, C_p decreases (that is, C_p increases numerically since C_p is negative here) as depth increases, as can be seen from Eq. (9a). On the other hand, if R is so large that the last two terms in Eq. (9) can be neglected, one obtains

$$C_p = -\frac{2gh}{U^2}\left(1 - \frac{\eta}{h}\right) \tag{10}$$

which is Laitone's result (cf. Ref. 4, p. 625, Eq. (6)) obtained by using a hydrostatic approximation. Laitone proceeds further to find the lower bound of η by considering the change in flow conditions across the hydraulic jump ($\eta = 1/2$ h, cf. Ref. 4, Eq. (5)) and thus claims a lower limit for C_p (cf. Ref. 4, Eq. (7)),

$$C_p \geq -gh\, U^{-2}\,. \tag{11}$$

Ausman's experimental results, Fig. 8, support this contention. While it is conceivable that this result holds for the limiting cases of low Froude number and large R, there must certainly be other instances of practical importance for which this result is incomplete. One would expect that in some cases the hydrodynamic effect overwhelms the hydrostatic effect completely. For example, if the Froude number is infinite, Eq. (9) reduces to

$$C_p = -\frac{2\eta}{R} \tag{12}$$

In this regard, a remark should be made on Laitone's contention that since his theoretical values of C_p agree with Ausman's experiments, they may be considered as confirming Ausman's result that the lift drops to zero as the surface is approached. In view of the present theory, which shows that Ausman's experiments are applicable only for low Froude numbers, it

should be clear that no such limitation on the force exists at higher Froude numbers. In fact it seems probable that, as the surface is neared, the hydrofoil lift approaches that of the equivalent planing surface, which is known to be greater than zero even in two dimensions. Further experiments along this line would be of interest.

IV. NEW MEASUREMENTS

In order to obtain experimental pressure distribution data over a wider range of parameters, a series of measurements were undertaken in the Free Surface Water Tunnel on two geometrically similar Joukowski hydrofoils at a fixed angle of attack $\alpha = 5^{o}$. The models and experimental technique are described in the Appendix while the main results of the present program are shown in Figs. 10 to 12. Figures 10 and 11 show the effect of Froude number, while Fig. 12 shows the effect of changing depth of submergence. These plots will now be discussed in more detail and compared with the preceding theory.

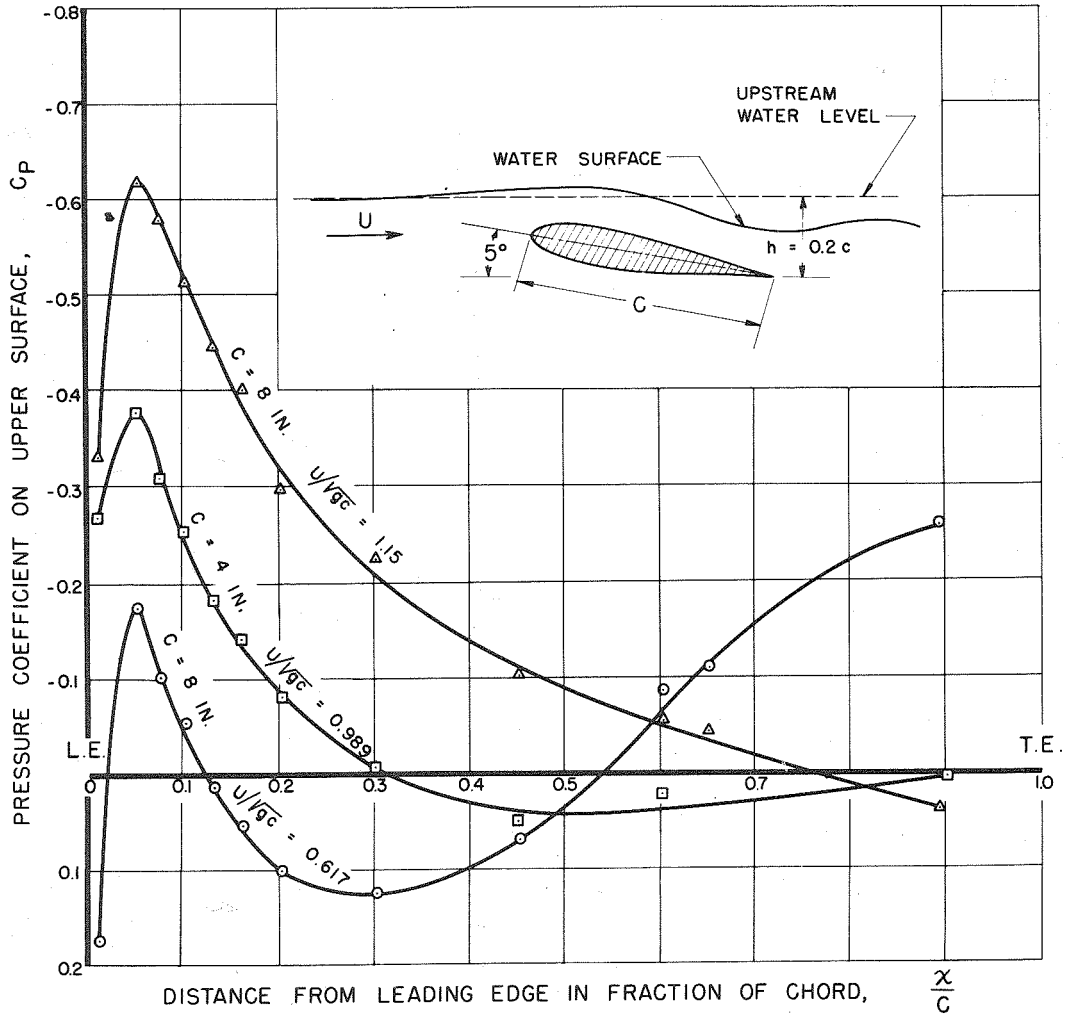

Fig. 10

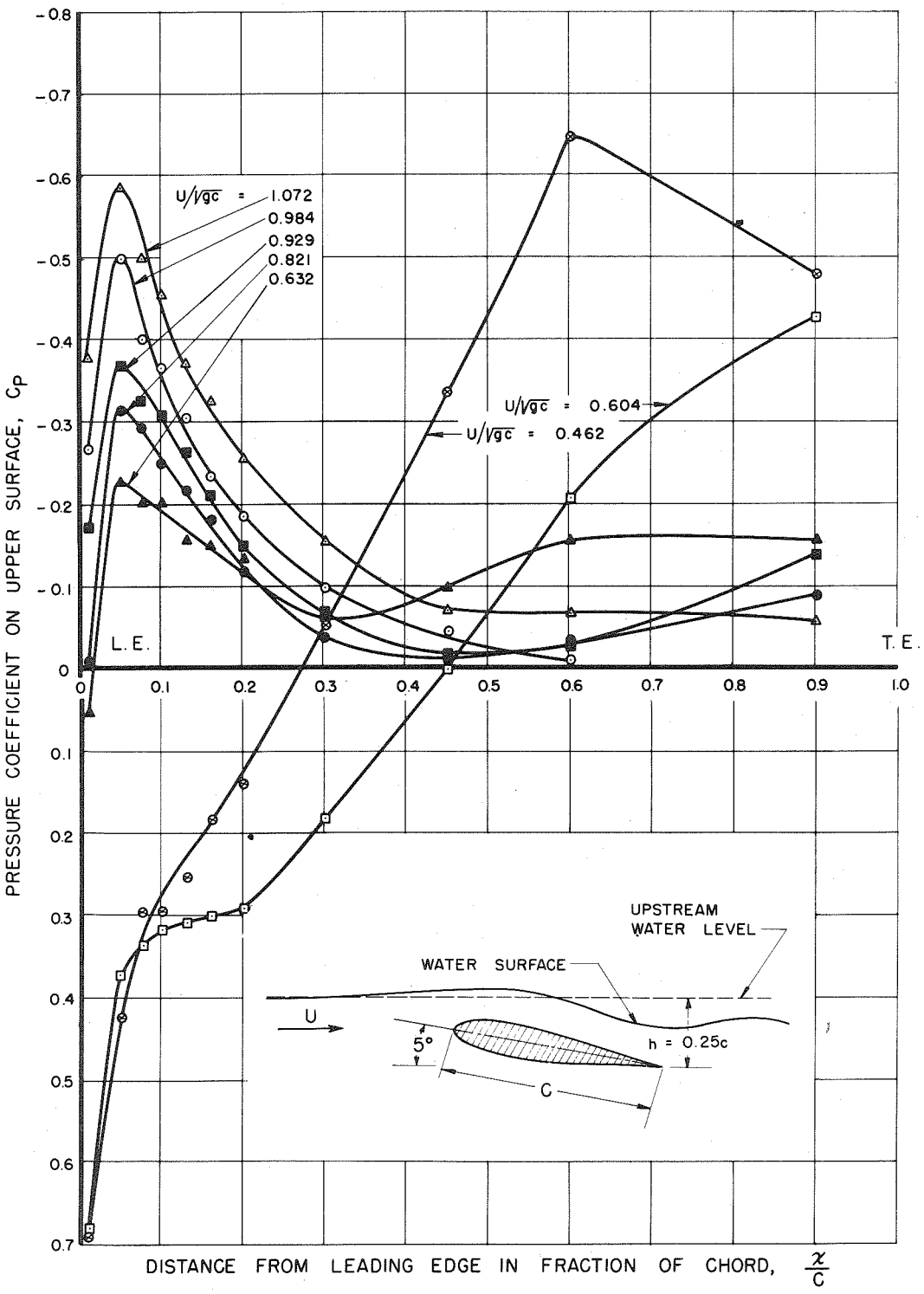
PRESSURE COEFFICIENT ON UPPER SURFACE, C_p
DISTANCE FROM LEADING EDGE IN FRACTION OF CHORD, $\frac{x}{C}$
$U/\sqrt{gc}$ = 1.072
0.984
0.929
0.821
0.632
$U/\sqrt{gc}$ = 0.604
$U/\sqrt{gc}$ = 0.462
L.E.
T.E.
UPSTREAM WATER LEVEL
WATER SURFACE
U
5°
h = 0.25c
C

Fig. 11a

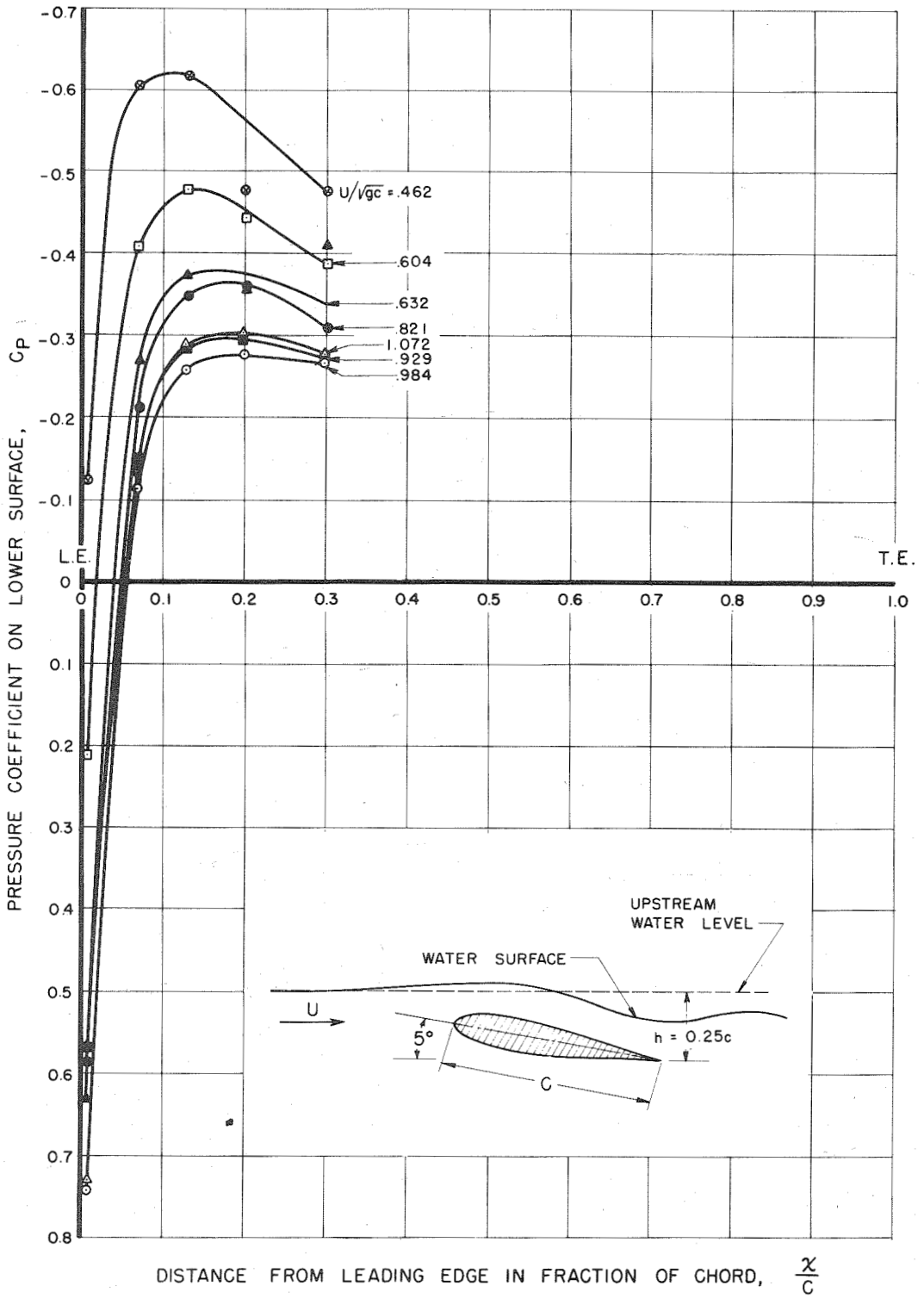
PRESSURE COEFFICIENT ON LOWER SURFACE, C_p
-0.7
-0.6
-0.5
-0.4
-0.3
-0.2
-0.1
0
0.1
0.2
0.3
0.4
0.5
0.6
0.7
0.8
L.E.
T.E.
0
0.1
0.2
0.3
0.4
0.5
0.6
0.7
0.8
0.9
1.0
$U/\sqrt{gc}$ = .462
.604
.632
.821
1.072
.929
.984
UPSTREAM
WATER LEVEL
WATER SURFACE
U
5°
h = 0.25c
C
DISTANCE FROM LEADING EDGE IN FRACTION OF CHORD, $\frac{x}{C}$

Fig. 11b

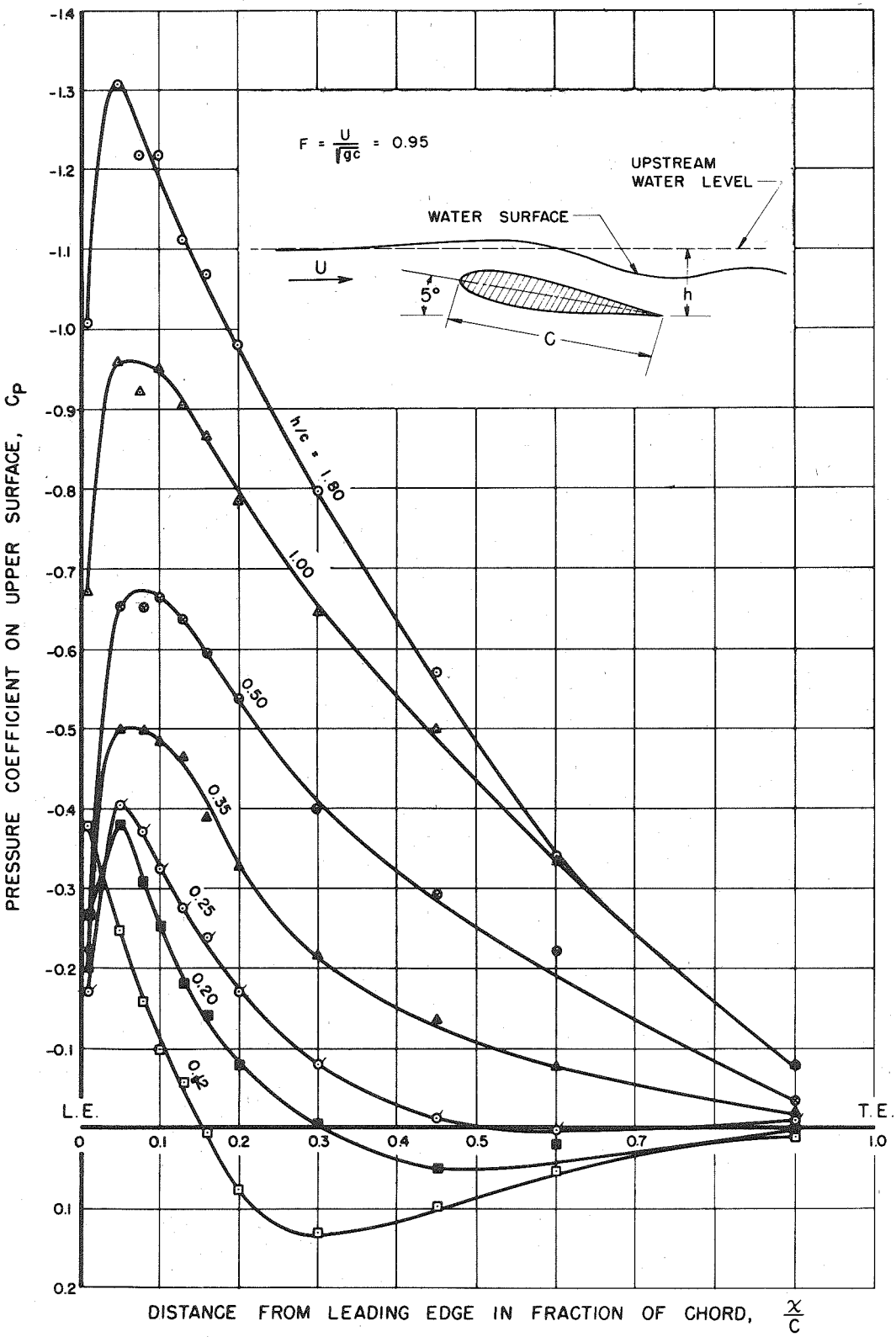
F = U/√gc = 0.95
UPSTREAM WATER LEVEL
WATER SURFACE
U
5°
h
C
h/c = 1.80
1.00
0.50
0.35
0.25
0.20
0.12
L.E.
T.E.
PRESSURE COEFFICIENT ON UPPER SURFACE, Cp
DISTANCE FROM LEADING EDGE IN FRACTION OF CHORD, x/C

Fig. 12

In Figs. 10 and 11 the effect of Froude number $U/\sqrt{gc}$ on the hydrofoil pressure is shown at a fixed attack angle and depth chord ratio h/c for two values of h/c. It will be noticed that a marked change takes place as the Froude number is decreased. The change is best shown for the case $h/c = 0.25$, Fig. 11, for which considerable data are available. At Froude numbers near 0.61 the whole character of the distribution changes. The peak negative pressure near the leading edge disappears and the pressure coefficient near the trailing edge is the lowest on the profile. This condition experimentally corresponds to the case where a hydraulic jump occurs on the hydrofoil (see Fig. 1b). Some simple tracer measurements showed that the flow at the trailing edge did not satisfy the Kutta condition for these runs. It is believed that these values of the parameters, especially the low Froude number, are beginning to correspond to Laitone's assumptions so that the pressure coefficient is indeed limited by his criterion, Eq. (11).

As the Froude number is increased, however, the pressure distributions look more nearly like those on a completely submerged hydrofoil. A peak in the negative pressure occurs near the leading edge. From there it drops monotonically toward the trailing edge. It is particularly significant that the negative peak is greater in magnitude the higher the Froude number. This trend is diametrically opposite from Laitone's criterion, Eq. (11), as perhaps can better be seen from Fig. 13 where the minimum pressure coefficients are plotted as a function of the parameter gh/U^2.

In Fig. 12 the effect of changing the depth chord ratio h/c at a fixed value of the Froude number $U/\sqrt{gc}$ can be seen. The Froude number shown is sufficiently high so that the pressure distribution behaves reasonably like that for deeply submerged profiles. The magnitude of the lowest pressure is reduced as the hydrofoil approaches the surface as one would expect from Eq. (11). When this data is cross-plotted against the parameter gh/U^2 as shown in Fig. 13, there appears at first sight to be more of a correlation with Laitone's criterion, but this, of course, is merely a coincidence corresponding to the manner in which the data was taken. A careful study of Fig. 13 will show that at high Froude numbers in the range of practical interest Eq. (11) is not sufficient to describe the behavior of the pressure, but must be replaced with the more general expression Eq. (9).

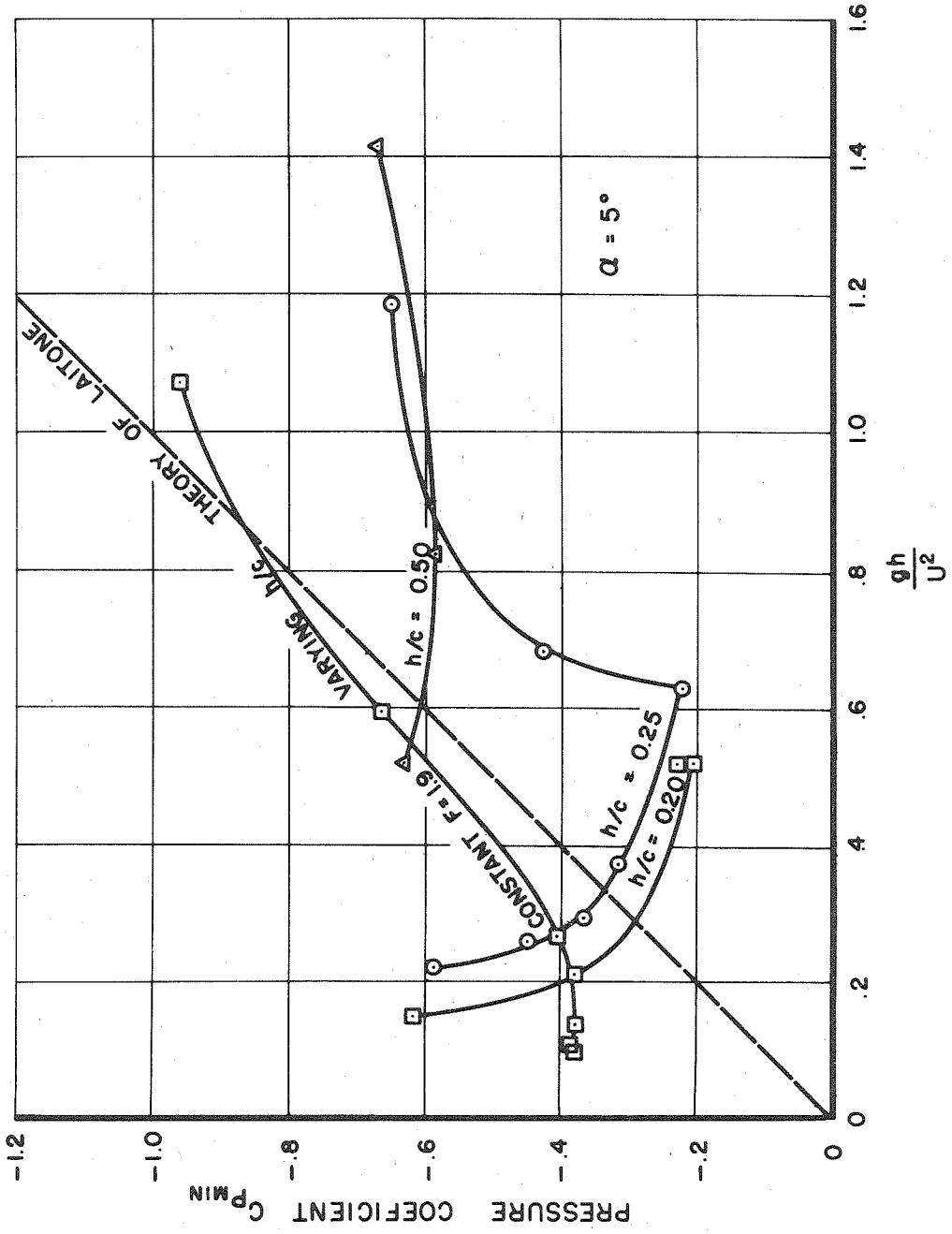
PRESSURE COEFFICIENT $C_{P_{MIN}}$
-1.2
-1.0
-.8
-.6
-.4
-.2
0
.2
.4
.6
.8
1.0
1.2
1.4
1.6
$\frac{gh}{U^2}$
$\alpha = 5°$
THEORY OF LAITONE
VARYING h/c
CONSTANT F=1.9
h/c = 0.50
h/c = 0.25
h/c = 0.20

Fig. 13

V. PRACTICAL APPLICATIONS

The preceding sections have shown in a qualitative way the important parameters which enter into the free surface effect on the hydrofoil pressure distribution. It is of interest to discuss now some of the practical applications of the results.

The relationship between parameters given in dimensionless form by Eq. (4) should be given due regard in future experimental work. It shows that for a given profile shape, the attack angle α, depth-chord ratio h/c, and the Froude number $U/\sqrt{gc}$ are the important experimental parameters. Thus, for example, if two hydrofoils of the same profile but different size are tested, the pressure distributions should be the same if α, h/c, and $U/\sqrt{gc}$ are the same. Any discrepancy would be an indication of extraneous influences, such as viscosity or channel boundary effect. The use of the Froude number is of course well-known and Eq. (4) is obviously only a means of expressing Froude's similarity criterion for gravity effects.

A problem of particular interest to the hydrofoil designer which involves the pressure distribution is the prediction of the speed of incipient cavitation. A program is now under way to study this problem and formulate practical methods of designing hydrofoils having a specified pressure distribution.[13] Since the methods employed to date take no account of the free surface, the question arises as to whether they give conservative results when applied to the design of a profile which will be run near the water surface. This question can be partly answered by the results of the preceding sections. Unless the craft is running at an extremely low Froude number, which is of course unlikely if cavitation is incipient, the first term of Eq. (9), representing the hydrodynamic effect, is the important one, and it shows that the incipient cavitation number is lower the nearer the hydrofoil runs to the surface. This may also be seen from Fig. 14, in which the negative peak pressures from Fig. 12 have been cross-plotted. Hence if the incipient cavitation number is known for the foil deeply submerged, one can expect that it will be lower for the foil near the surface. It is, therefore, seen that the method based on a completely submerged foil will, in fact, be conservative.

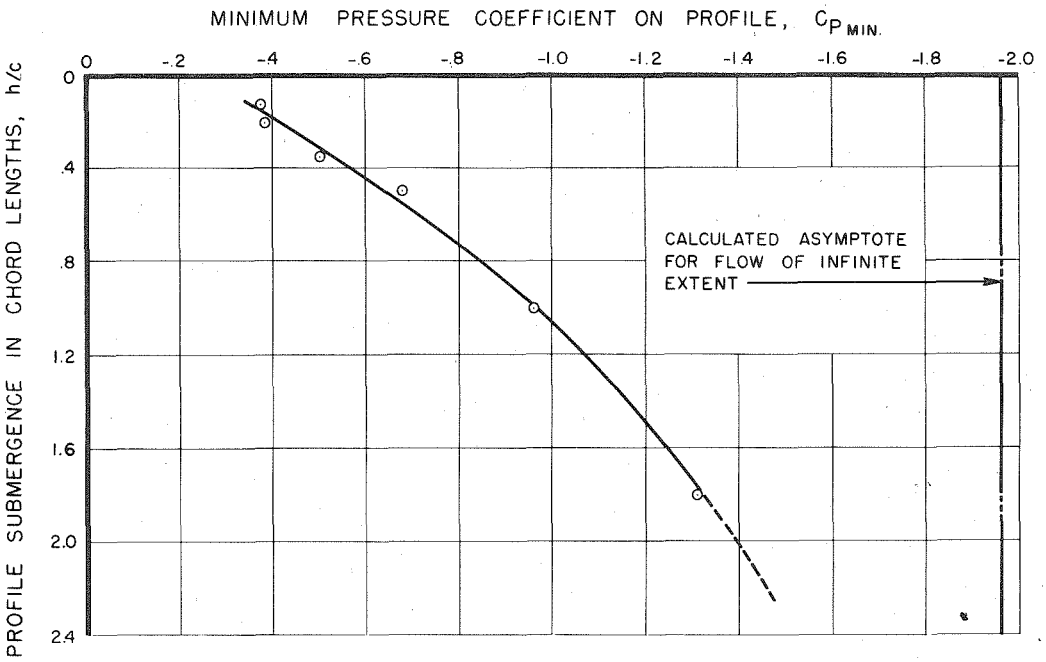

Fig. 14

It would be of great interest, of course, to obtain more quantitative information on the free surface effects to enable the designer to make somewhat more precise estimates. Practical hydrofoils mounted on boats will probably never approach the surface so closely as the ones in the preceding experiments because of the danger of suddenly breaking through the free surface. Surface waves increase this danger. Corrections, therefore, for the effect of the free surface may not be very large and relatively simple methods may suffice to predict them.

VI. CONCLUDING REMARKS

In the preceding sections the effect of the free surface on hydrofoil pressure distributions has been analyzed both theoretically and experimentally. It seems clear that the results confirm the point of view, already expressed by many workers, that hydrofoils running near the surface can be studied analytically within the framework of the usual potential theory. The application of such theory to hydrofoils is still in its infancy and there are a large number of practical problems on which it should be brought to bear. Further, the experience of workers in aerodynamics has long since proven the value of basic experimental work to compare with the theory and to suggest new assumptions and approaches. The writers hope that the effort along these lines made here will prove of value to those who work on these interesting problems in the future.

APPENDIX A

Experimental Technique

The purpose of this Appendix is to describe in detail the apparatus and techniques used in the measurements of pressure distributions.

Models

The hydrofoil sections used in these experiments were 12% thick symmetrical Joukowski profiles with thickened trailing edges. Two models, of chord length 4 and 8 inches, were used. Both hydrofoils had a span of 14 inches. These models were originally designed for high-speed water tunnel experiments on cavitation scale effect,[14] with the result that the pressure taps in these models allowed for pressure surveys to be made only on the upper surfaces of the two hydrofoils. Although this tap arrangement precluded the determination of profile lift, it was satisfactory for measuring pressure distributions over the upper surfaces and around the noses of the profiles. Scale drawings of the two profiles and of the pressure tap locations for each model are shown in Fig. 15.

Water Tunnel

With the exception of a few preliminary tests which were performed in the flume of the Soil Conservation Laboratory, the experiments described herein were carried out using the Free Surface Water Tunnel.[15, 16] This tunnel is of the closed circuit type, powered by a 75 h.p. electric motor. The working section is 8 ft long by 20 in. wide by 19 in. deep. In the vast majority of work done previously in this tunnel, the velocity has been of the order 8 to 27 fps which is greater than the so-called critical speed given by the channel wave velocity $U_{wave} = \sqrt{gh}$, where h is the channel depth. Thus for a channel depth of 19 inches, the critical speed is 7.2 fps.

For the purposes of the present experiments it was convenient* to operate the tunnel at sub-critical velocity, that is, less than 7.2 fps. After a little preliminary experimentation it was found that a uniform flow without appreciable wave disturbances on the surface could be obtained up to

*Since Ausman[3] and Laitone[4] have raised some questions about the validity of super-critical testing, the writers felt that it would avoid controversy if the present tests were run at sub-critical speeds.

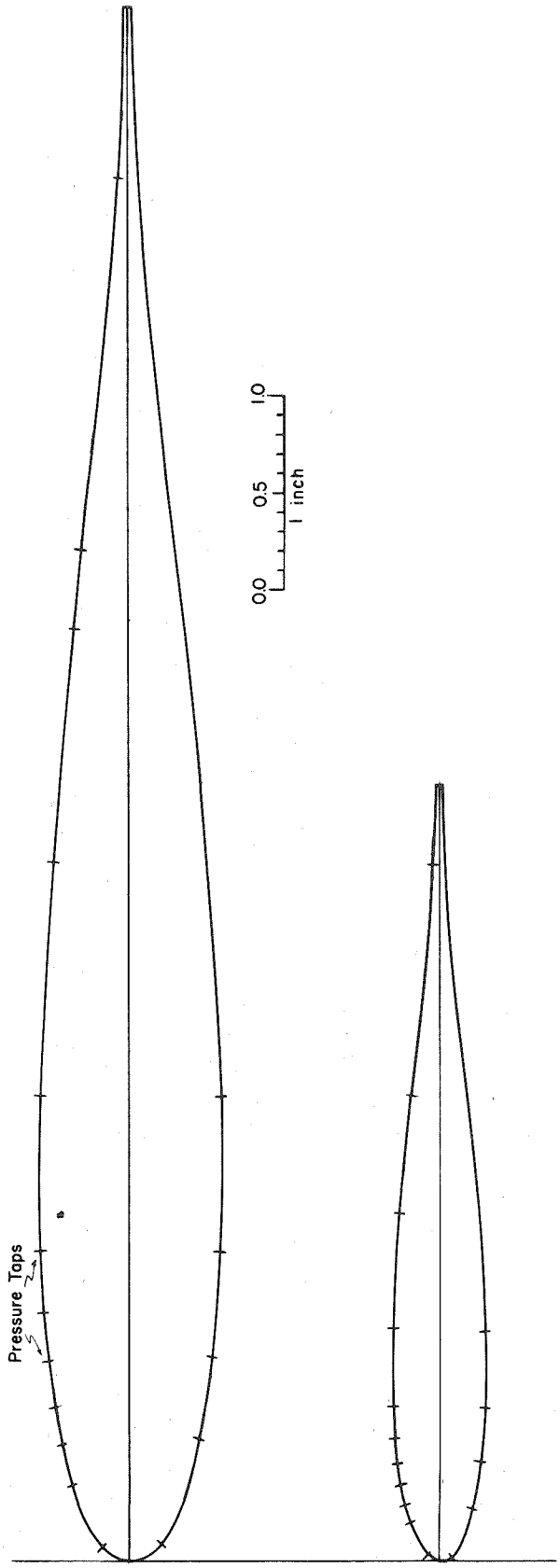

Fig. 15

four feet per second. If slight surface disturbances could be tolerated, as was the case in some tests, speeds as high as 5.5 fps could be obtained. When operated at these speeds it was found that the tunnel performed best if run in such a manner that a free surface existed upstream of the working section to the elbow; that is, the flow in the nozzle was not deep enough to contact the top boundary wall of the nozzle. When so run, the tunnel does not change speed independently of the water depth so that for each speed the water level must be adjusted by the addition or removal of water from the storage reservoir. This causes no great inconvenience since it is simple enough to run all the tests corresponding to a given speed at once.

It should be noted that even though the tests are run at sub-critical speed the channel wave effects cannot always be completely ignored. Thus, if a foil is inserted in the working section when the tunnel is running very near critical velocity, it will excite spurious waves which in turn influence the pressures and forces. Nearly all the tests therefore were run at speeds below 4 fps to avoid such errors. The same principle of course applies to running tests at super-critical speeds such as have commonly been undertaken in this tunnel, so that one usually runs at appreciably higher speeds than critical.

Velocity Measurements

Velocities were measured with a Prandtl tube and several velocity surveys were made near the point where the foil was placed. The deviations from a rectangular velocity profile were found to be negligible, except possibly near the surface. The discrepancies here, however, were not necessarily significant since a Prandtl probe does not read correctly very near the surface. So far as the writers know, calibration data for a Prandtl probe near the surface are not available.

Instrumentation

Pressure measurements were made using standard pressure tap and tubing techniques and the pressure signal measured with a Statham strain gage transducer. The strain gage was wired as one leg of a bridge circuit and the bridge balanced using a vacuum tube voltmeter as a null indicator. The arrangement is shown schematically in Fig. 16. The gage calibration was checked several times during the experiments but no detectable drift was found. In general, the accuracy of the Statham gage and its associated

electronic instrumentation appeared to be very good, much better in fact than necessary for this test. Errors due to air bubbles in the lines were believed to have been mostly eliminated by making check readings with the tunnel not running. When so measured, all taps should give the same reading, and hence this source of error could be quickly checked. The Statham gage was also used to measure the velocity head with an appropriate valve and manifold arrangement as shown in Fig. 16.

Experimental Setup

The foils were mounted between two end plates as shown in Fig. 17, to create a two-dimensional flow. Actual check measurements between the plates with the foil removed showed that the lateral variation in the velocity was negligible except, of course, in a thin boundary layer near each plate. The plates were mounted on a tunnel-elevating mechanism so that they could be adjusted vertically. Photographs of the experimental setup are shown in Figs. 18 and 19.

In a typical run the foil was lowered on a calibrated elevating mechanism until its trailing edge was a known distance below the undisturbed position of the free surface, which was measured by a point gage about two feet upstream of the model. The flow velocity was then measured by inserting the Prandtl probe upstream of the model. The Prandtl probe was then removed and the various pressure taps read in turn after which the Prandtl probe was reinserted to check the velocity. If the velocity had varied appreciably (over 2%), the tests were rerun. Also in a number of cases complete check runs were made on different days without detecting more than a few percent discrepancy.

Photographs

In the course of some preliminary experiments, photographs such as Figs. 1 to 5 were taken of the 8-inch foil with one end plate removed and the end of the foil held against the tunnel window as shown in Fig. 20. Thus, it was possible to obtain a photographic record showing clearly the type of wave phenomena encountered. No pressure measurements were taken with the foil supported in this fashion since the alignment was not believed to be very precise.

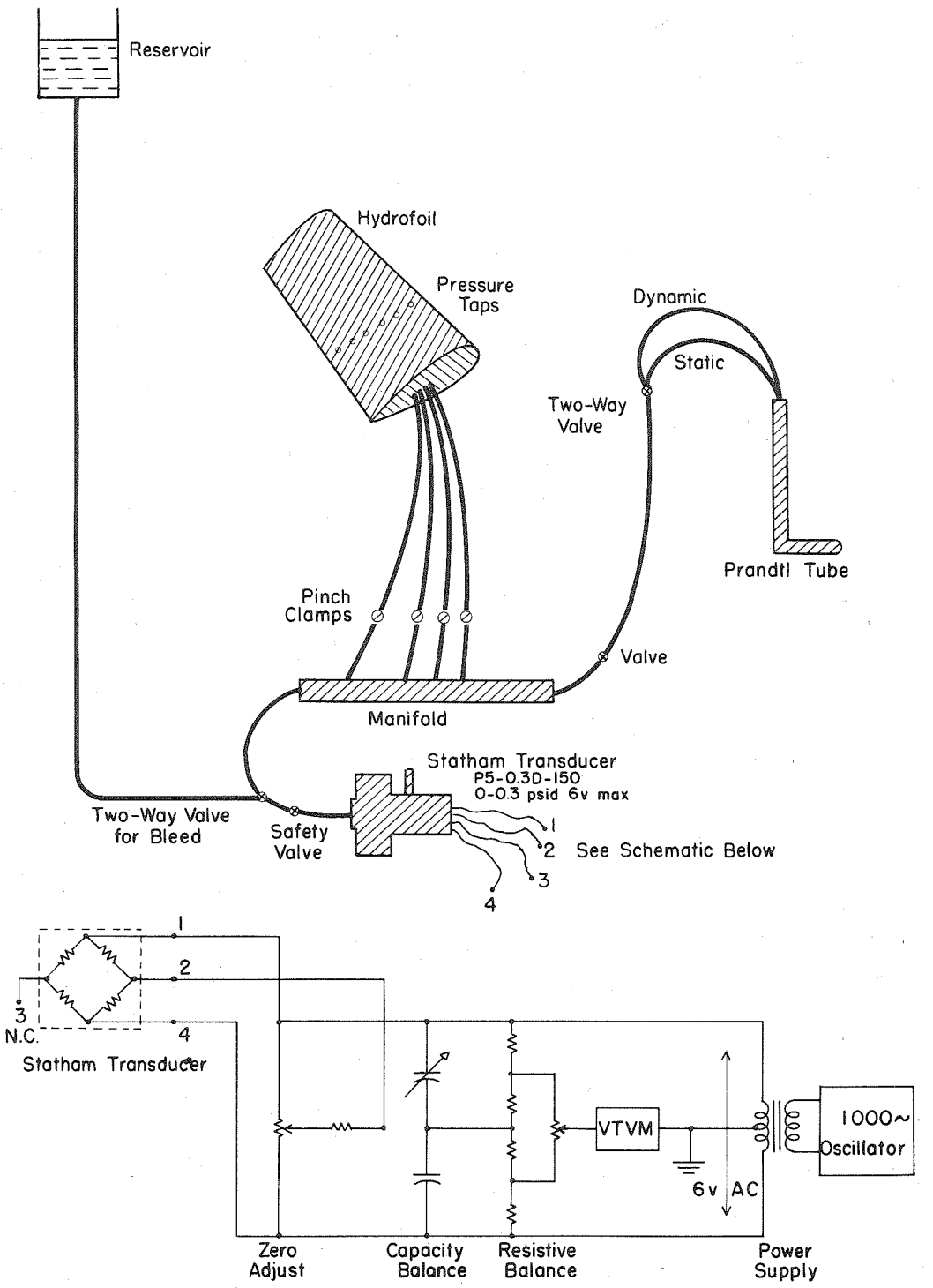
Reservoir
Hydrofoil
Pressure Taps
Dynamic
Static
Two-Way Valve
Prandtl Tube
Pinch Clamps
Valve
Manifold
Statham Transducer
P5-0.3D-150
0-0.3 psid 6v max
Two-Way Valve for Bleed
Safety Valve
1
2
3
4
See Schematic Below
1
2
3
N.C.
4
Statham Transducer
VTVM
1000~ Oscillator
6v AC
Zero Adjust
Capacity Balance
Resistive Balance
Power Supply

Fig. 16

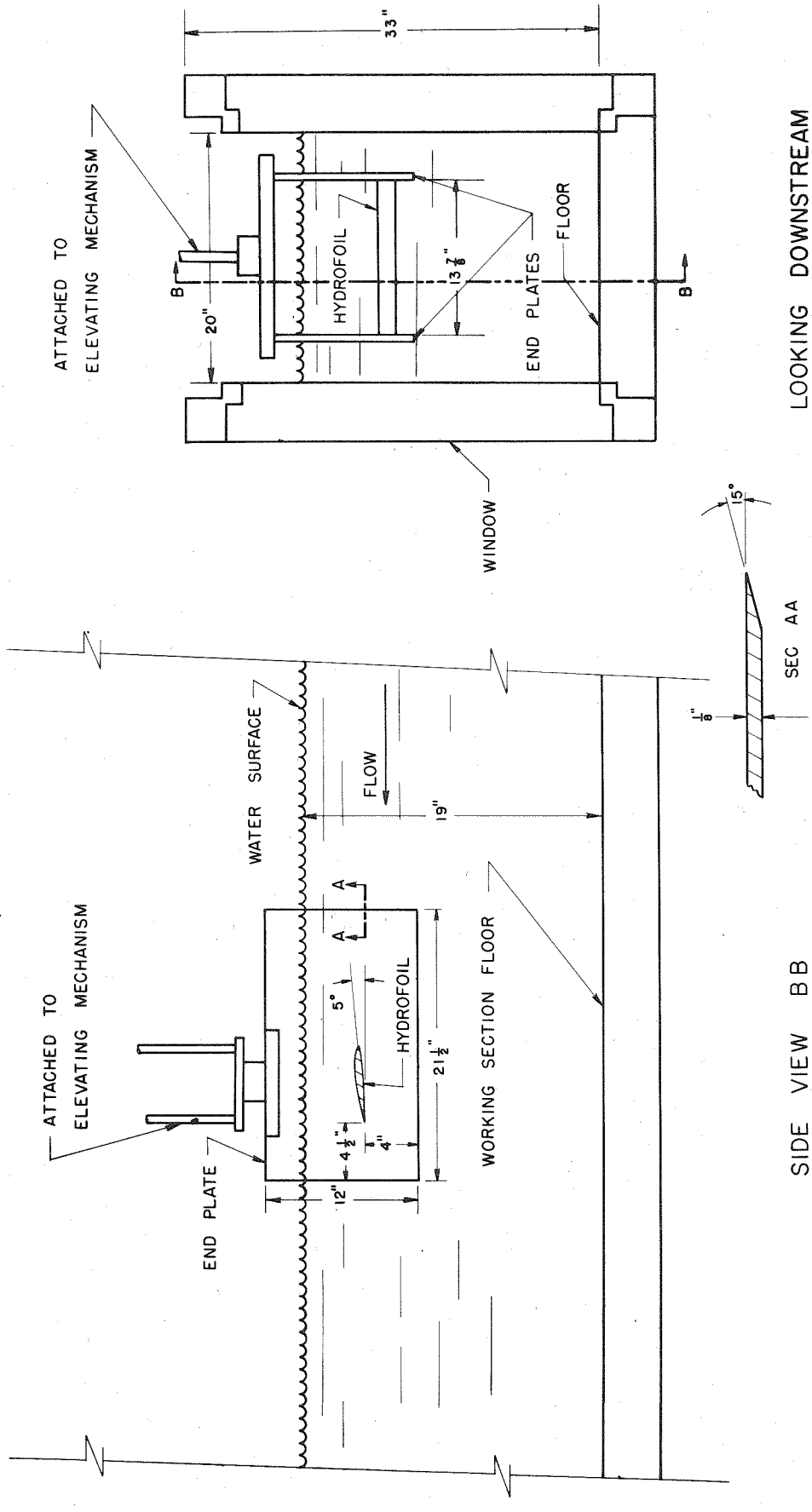
ATTACHED TO
ELEVATING MECHANISM
33"
B
20"
HYDROFOIL
13 7/8"
END PLATES
FLOOR
B
WINDOW
LOOKING DOWNSTREAM
15°
SEC AA
1/8"
WATER SURFACE
FLOW
19"
A
A
5°
HYDROFOIL
21 1/2"
4 1/2"
4"
12"
END PLATE
WORKING SECTION FLOOR
SIDE VIEW BB

Fig. 17

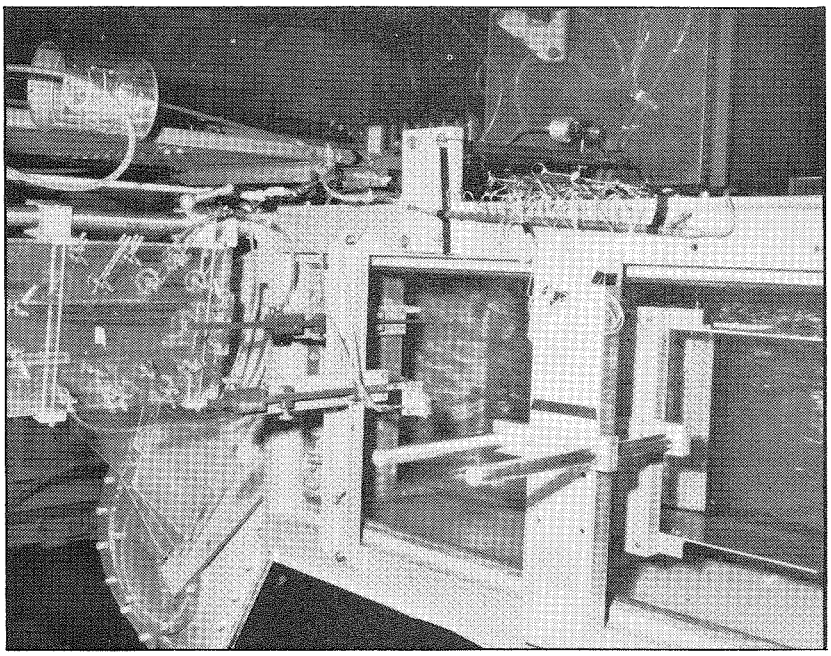

Fig. 19

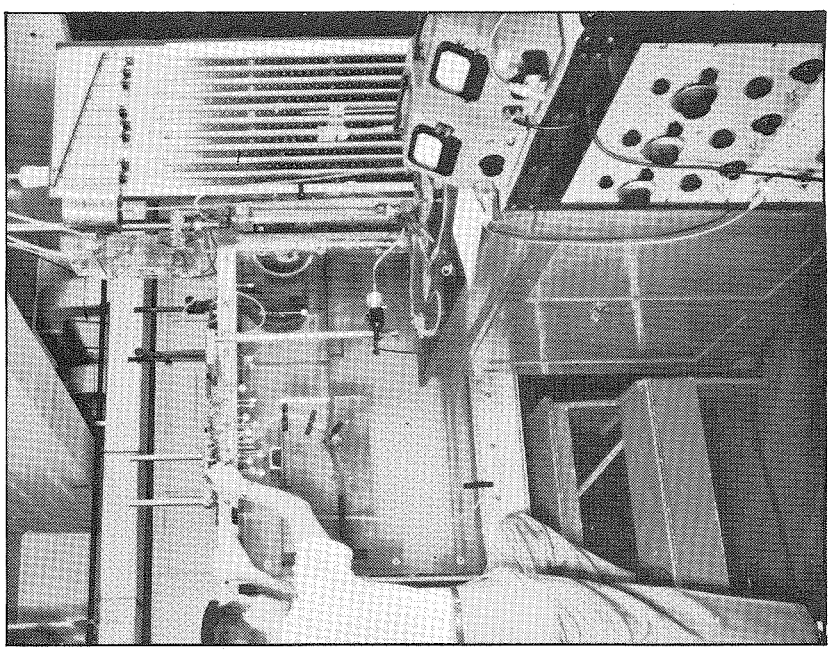

Fig. 18

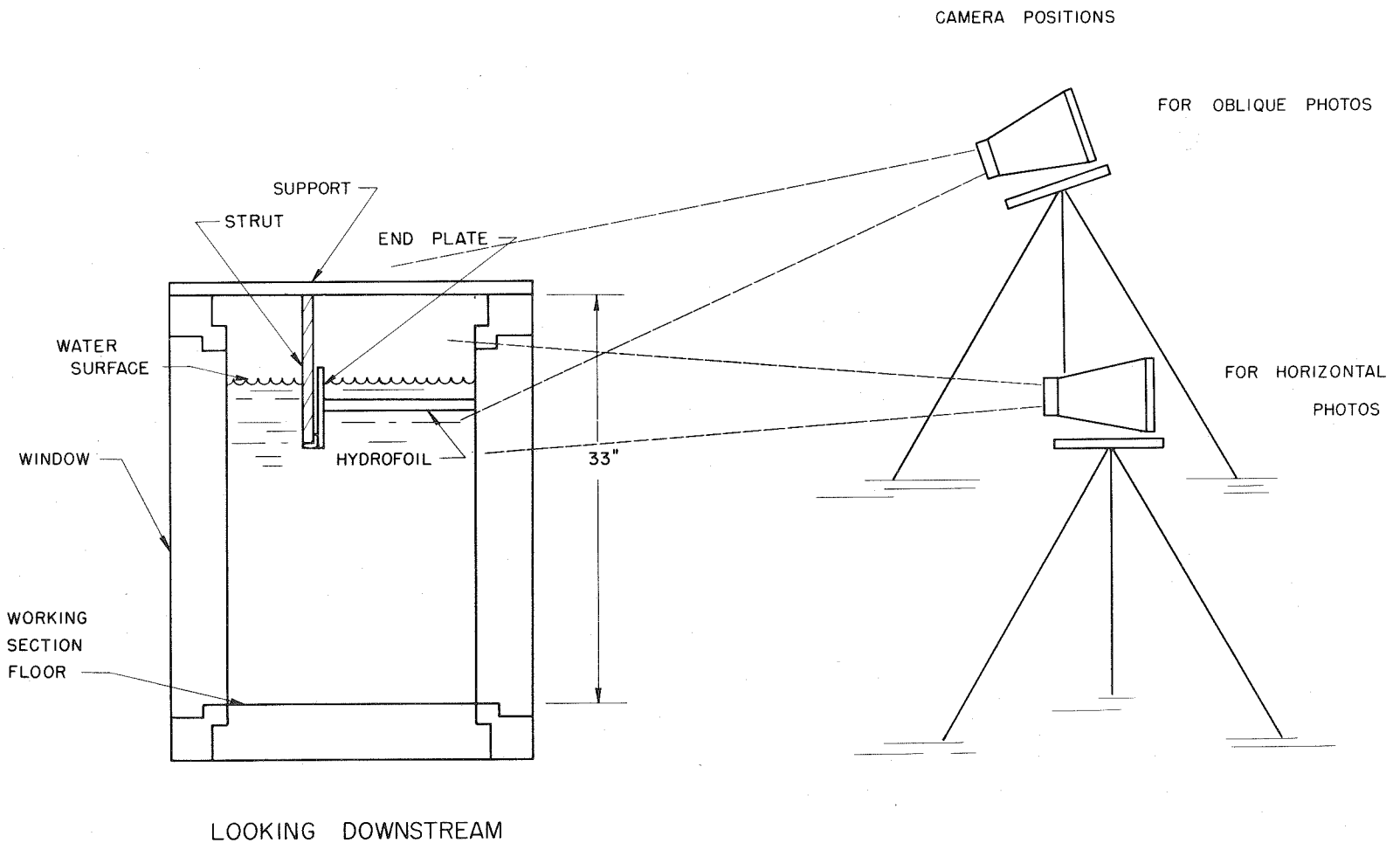
CAMERA POSITIONS
FOR OBLIQUE PHOTOS
SUPPORT
STRUT
END PLATE
WATER SURFACE
WINDOW
HYDROFOIL
33"
FOR HORIZONTAL PHOTOS
WORKING SECTION FLOOR
LOOKING DOWNSTREAM

Fig. 20

APPENDIX B

Computation of Lift and Drag for a Specific Hydrofoil

The purpose of this Appendix is to give some of the details of the computations for a specific hydrofoil of finite span which lead to the theoretical curves shown in Fig. 6. The starting point for the present numerical example is the calculation for a specific hydrofoil which was carried out in Ref. 9. The hydrofoil was taken to have an elliptic distribution of lift, an elliptic plan form of span-chord ratio 5 and aspect ratio 6.3, a fixed geometric angle of attack of 6° and a chord length of 8 ft. The speed was assumed to be 100 fps which corresponds therefore to a Froude number $U/(gc)^{1/2}$ of 6.23. The results of this computation are shown as Fig. 6 of Ref. 9, in which, however, no skin friction drag has been included.

The skin friction drag may be estimated for the experimental Reynolds number by using the Prandtl and Schlichting formula[17]

$$C_f = 0.455\,(\log_{10} R_e)^{-2.58}\,.$$

Since both surfaces of the hydrofoil must be accounted for, the value of the skin friction drag coefficient for the hydrofoil will be approximately twice this magnitude, that is $C_{Df} = 2C_f$. For the experiments used in the comparison here, the Reynolds number was about 654,000, so that a value of $C_{Df} = 0.011$ was added to the induced and wave drag coefficient previously computed. The final result is shown as the curve of drag coefficient C_D labeled "theory" in Fig. 6 of the present report.

The experimental points shown in Fig. 6 were cross-plotted from NACA towing tank data found in Ref. 10. The hydrofoil used in the tests had a 5 in. chord and was an NACA 23012, of rectangular plan form and aspect ratio 6. The attack angle was 6° and the towing speed was approximately 20 fps, corresponding to a Froude number $U/\sqrt{gc}$ of 5.45 and a Reynolds number of 654,000. Although the plan form and Froude number for the theoretical example are slightly different from these experimental values, the comparison can still be expected to be valid since the effect of plan form is small and moreover the theory predicts that the discrepancy due to the difference in Froude number should be negligible for the present range of Froude number. In any event, these small errors could be calculated if so

desired. It will be seen, however, from Fig. 6 where the theoretical and experimental values are plotted for comparison, that the agreement is very good.

APPENDIX C

Notation

(Note: Much of the notation is defined on Fig. 9).

c	hydrofoil chord length
C_p	pressure coefficient, defined by Eq. 4
$C_{p\,min}$	minimum value of pressure coefficient on upper surface of hydrofoil
F	Froude number, $F = U/\sqrt{gc}$
g	acceleration due to gravity
h	submergence of trailing edge below undisturbed free surface
n	curvilinear coordinate measured normal to stream filament
p	pressure anywhere in fluid
p_u	pressure at some point (x_u, y_u) on upper surface of hydrofoil
q	velocity anywhere in fluid
q_f	velocity along free surface
q_u	velocity at some point (x_u, y_u) on upper surface of hydrofoil
r	radius of curvature of streamline
R	radius of curvature at some point (x_u, y_u) on upper surface of hydrofoil
s	curvilinear coordinate measured along a stream filament
U	uniform flow velocity at infinity
x	rectangular coordinate
y	rectangular coordinate
y_u	y-coordinate of upper surface of hydrofoil
α	geometrical angle of attack
η	depth of flow over hydrofoil
ρ	fluid density

REFERENCES

1. Buerman, T.M., Leehey, P., and Stilwell, J.J., "An Appraisal of Hydrofoil Supported Craft", Trans. of the Society of Naval Architects and Marine Engineers, Vol. 61, pp. 242-279 (1953).

2. Ausman, J.S., "Experimental Investigation of the Influence of Submergence Depth Upon the Wave-Making Resistance of an Hydrofoil", Master of Science Thesis, University of California, Berkeley, 1952.

3. Ausman, J.S., "Pressure Limitation on the Upper Surface of a Hydrofoil", Doctor of Philosophy Thesis, University of California, Berkeley, 1953.

4. Laitone, E.V., "Limiting Pressure on Hydrofoils at Small Submergence Depths", J. of Appl. Phys. Vol. 25, No. 5, p. 623, May 1954.

5. Green, A.E., Proc. Camb. Phil. Soc., 32 (1936). See also Milne-Thomson, L.M., "Theoretical Hydrodynamics", Second Edition, MacMillan, London 1949, p. 297.

6. Keldysh, M.V. and Lavrentiev, M.V., "On the Motion of an Aerofoil under the Surface of a Heavy Fluid, i.e., a Liquid", ZAHI paper, Moscow, Jan. 1935. For English translation see Science Translation Service, Cambridge, Mass., STS-75, Nov. 1949.

7. Weinig, F., "On the Theory of Hydrofoils and Planing Surfaces", NACA TM 845 (1938). Translated from Luftfahrtforschung, Vol. 14, No. 6, June 1937.

8. Wladimirow, A., "Approximative Hydrodynamic Calculation of a Hydrofoil of Finite Span", ZAHI Rep. No. 311 (1937) Moscow. (English translation available, Central Air Documents Office No. ATI-57689).

9. Wu, Y.T., "A Theory for Hydrofoils of Finite Span", J. of Math. and Phys., Vol. 33, No. 3, Oct. 1954, p. 207. See also _____, "A Theory for Hydrofoils of Finite Span", California Institute of Technology, Hydrodynamics Laboratory Report No. 26-8, May 1953.

10. Ward, K.E. and Land, N.S., "Preliminary Tests in the N.A.C.A. Tank to Investigate the Fundamental Characteristics of Hydrofoils", NACA Wartime Rept. L-766 (1940).

11. Bakhemeteff, B.A., "Hydraulics of Open Channels", McGraw-Hill Book Company, Inc., New York, 1932.

12. Rouse, H., "Fluid Mechanics for Hydraulic Engineers", McGraw-Hill Book Co. Inc., New York, 1938.

13. Parkin, B.R. and Peebles, G.H., "Calculation of Hydrofoil Sections from Prescribed Pressure Distributions", California Institute of Technology, Hydrodynamics Laboratory Report (to be released).

REFERENCES (Continued)

14. Parkin, B.R., "Scale Effects in Cavitating Flow - A Preliminary Report", California Institute of Technology, Hydrodynamics Laboratory Report No. 21-7, 1951.

15. Knapp, R.T., Levy J., O'Neill, J.P., and Brown, F.B., "The Hydrodynamics Laboratory of the California Institute of Technology", Trans. A.S.M.E., p. 437, July 1948.

16. O'Neill, J.P., "The Hydrodynamics of the Free-Surface Water Tunnel", California Institute of Technology, Hydrodynamics Laboratory Report No. N-65, 1949.

17. Schlichting, H., "Lecture Series - Boundary Layer Theory, Part II - Turbulent Flows", NACA TM 1218, p. 39 (1949).

DISTRIBUTION LIST FOR TECHNICAL REPORTS ISSUED UNDER CONTRACT NONR-220(12)

Item	Address	No. Copies
1	Commanding Officer and Director, David Taylor Model Basin, Washington 7, D.C., Attn: Code 580	21
2	Chief of Naval Research, Office of Naval Research, Department of the Navy, Washington 25, D.C., Attn: Mechanics Branch (Code 438)	6
3	Commanding Officer, Branch Office, Office of Naval Research, 495 Summer St., Boston 10, Mass.	1
4	Commanding Officer, Branch Office, Office of Naval Research, 346 Broadway, New York 13, N.Y.	1
5	Commanding Officer, Branch Office, Office of Naval Research, The John Crerar Library Bldg., 10th Floor, 86 E. Randolph St., Chicago 1, Ill.	1
6	Commanding Officer, Branch Office, Office of Naval Research, 1000 Geary St., San Francisco 9, Calif.	1
7	Commanding Officer, Branch Office, Office of Naval Research, 1030 E. Green Street, Pasadena 1, Calif.	2
8	Asst. Naval Attache for Research, Office of Naval Research, American Embassy, London, England, Navy 100, F.P.O. New York, N.Y.	2
9	Director, Naval Research Laboratory, Office of Naval Research, Washington 25, D.C. Attn: Librarian	9
10	Bureau of Aeronautics, Dept. of the Navy, Washington 25, D.C., Attn: Aero and Hydro Branch (Code AD3)	2
11	Bureau of Ordnance, Dept. of the Navy, Washington 25, D.C., Attn: Code Re9 Code Re6 Code Re3	1 1 1
12	Commander, U.S. Naval Ordnance Laboratory, U.S. Navy Bureau of Ordnance, White Oak, Silver Spring 19, Maryland	2
13	Underwater Ordnance Dept., Naval Ordnance Test Station, 3202 E. Foothill Blvd., Pasadena, Calif., Attn: Pasadena Annex Library (Code P 5507)	3
14	Chief, Bureau of Ships, Dept. of the Navy, Washington 25, D.C., Attn: Technical Library (Code 312) for additional distribution to:	10

Distribution List (continued)

Item	Address	No. Copies
	(Bureau of Ships distribution) Research and Development (Code 300) Ship Design (Code 410) Preliminary Design (Code 420) Hull Design (Code 440) Hull Scientific (Code 442) Propeller Design (Code 554)	
15	Mr. R. H. Kent, Ballistic Research Laboratories, Dept. of the Army, Aberdeen Proving Ground, Maryland	1
16	Director of Research, National Advisory Committee for Aeronautics, 1512 H Street, N.W., Washington 25, D.C.	1
17	Director, Langley Aeronautical Lab., National Advisory Committee for Aeronautics, Langley Field, Virginia	1
18	Commander, Naval Ordnance Test Station, Inyokern, China Lake, Calif., Attn: Library (Code 5507)	1
19	Dr. K.S.M. Davidson, Experimental Towing Tank, Stevens Institute of Technology, Hoboken, N. J.	1
20	Dr. J.H. McMillen, National Science Foundation, 1520 H Street, N.W., Washington 25, D.C.	1
21	Dr. A. Miller, Bureau of Ordnance (Code Re3d) Navy Dept. Washington 25, D.C.	1
22	Dr. H. Rouse, Iowa Institute of Hydraulic Research, State University of Iowa, Iowa City, Iowa	1
23	Dr. R.G. Folsom, Director, Engineering Research Institute, University of Michigan, East Engineering Bldg. Ann Arbor, Michigan	1
24	Dr. V.L. Streeter, Engineering Dept., University of Michigan, Ann Arbor, Michigan	1
25	Dr. G.F. Wislicenus, Pennsylvania State University, Ordnance Research Laboratory, University Park, Pa.	1
26	Dr. A.T. Ippen, Dept. of Civil and Sanitary Engineering, Massachusetts Institute of Technology, Cambridge 39, Mass.	1
27	Dr. L.G. Straub, St. Anthony Falls Hydraulic Laboratory, University of Minnesota, Minneapolis 14, Minn.	1
28	Prof. K.E. Schoenherr, University of Notre Dame, College of Engineering, Notre Dame, Indiana	1
29	Director, Ordnance Research Laboratory, Pennsylvania State University, University Park, Pa.	1

Distribution List (continued)

Item	Address	No. Copies
30	Society of Naval Architects and Marine Engineers 74 Trinity Place, New York 6, N.Y.	1
31	Prof. J.K. Vennard, Stanford University, Dept. of Civil Engineering, Stanford, California	1
32	Prof. J.L. Hooper, Worcester Polytechnic Institute, Alden Hydraulic Laboratory, Worcester 6, Mass.	1
33	Prof. J.M. Robertson, Dept. of Theoretical and Applied Mechanics, University of Illinois, Urbana, Ill.	1
34	Dr. A.B. Kinzel, President, Union Carbide and Carbon Research Lab., Inc., 30 E. 42nd St., New York, N.Y.	1
35	Goodyear Aircraft Corp., Akron 15, Ohio, Attn: Security Officer	1
36	Prof. H.R. Henry, Hydraulics Laboratory, Michigan State College, East Lansing, Michigan	1
37	British Joint Services Mission, Navy Staff: Via Chief, Bureau of Ordnance, Navy Dept., Washington 25, D.C. Attn: Code AD8	9
38	Commander, Submarine Development Group TWO, Box 70, U.S. Naval Submarine Base, New London, Conn.	1
39	Commanding Officer and Director, U.S. Navy Engineering Experiment Station, Annapolis, Maryland	1
40	Library of Congress, Washington 25, D.C., Attn: ASTIA	1